A Review on Synthetic Methods of Nanostructured Materials

Ayuk Eugene L[1], Ugwu Mariagoretti O[1], Aronimo Samuel B[2]

[1]Chemical Sciences Department, Faculty of Natural and Applied Sciences, Godfrey Okoye University, Ugwuomu –Nike, Enugu, Nigeria
[2]Department of Chemistry Kogi State College of Education (Technical) Kabba, Kogi State, Nigeria
Corresponding Author: eugeneayuk@yahoo.com

Abstract Interest in Nanoscience and Nanomaterials has remained unabated and has attracted so much attention in recent times. New advances both in the preparation and device fabrication have emerged due the development of nano and material sciences. Scientists from different fields of research such as biologists, chemists, physicists, material scientists, pharmacists and engineers are involved in this venture. This is because Nanoparticles (NPs) have very wide range of applications in areas like health care, cosmetics, food and feed, environmental health, mechanics, optics, biomedical sciences, chemical industries, electronics, space industries, drug-gene delivery, energy science, optoelectronics, catalysis, single electron transistors, light emitters, nonlinear optical devices, as well as photo electrochemical applications. The synthesis of nanomaterials is an important milestone in the pursuit. A lot of significant developments have been made in the improvement of methods of synthesis of nanomaterial by chemists, materials scientists and engineers. In this review various methods of fabricating nanomaterials are discussed. They include Mechanical ball milling, Mechanochemical method, Etching techniques, Sputtering, Laser Ablation, Gas Condensation, Vacuum Deposition and Vaporization, Chemical Vapor Deposition (CVD) and Chemical Vapor Condensation (CVC), Electrodeposition, Chemical Precipitation, Sol-Gel Techniques, Sonochemical method, Theromolysis of metal complexes, Microwave synthesis, Electrochemical method and Biological method.

Keywords Nanoscience, nanomaterials, material science, nanofibres, nanowires, nanotubes, top-down, bottom-up

1. Introduction

Nanotechnology as an important field of modern research deals with the designing, synthesis, and manipulation of particle structures ranging from approximately 1-100 nm in size. Nanoparticles (NPs) have wide applications in areas like health care, cosmetics, food and feed, environmental health, mechanics, optics, biomedical sciences, chemical industries, electronics, space industries, drug-gene delivery, energy science, optoelectronics, catalysis, single electron transistors, light emitters, nonlinear optical devices, as well as photo electrochemical applications [1-7]. Interest in nanotechnology has been sustained due to the wide range of applications of nanostructured materials, with dimensions, which include grain size, layer thickness or shapes below 100 nm as mentioned above. Nanomaterials are observed in Nanostructured materials such as Nanoparticles, Nanocomposites, Nanocapsules, Nanoporous materials, Nanofibres, Fullerenes, Nanowires, Single-Walled and Multi-Walled (Carbon) Nanotubes and Molecular Electronics [7]. These groups of materials exhibit wide range of electronic, magnetic, mechanical or optical properties and have been used to develop products of industrial and domestic importance. For instance,

magnetic nanoparticles with several ultra-thin layers have been employed in the development of advanced data storage devices [8].

However, one of the main factors in nanoscience has to do with the synthesis of these nanomaterials since they exhibit properties which differ from those of bulk materials and has been discovered that optical, magnetic and electrical properties are sensitive to size effects [9]. In addition, nanosized particles are also very efficient especially in the field of catalysis due to the high ratio of surface to volume they posses [10]. In order to tackle the issue of size control, morphology, structure and chemical composition, different processes of nanomaterials synthesis have been investigated and large numbers of studies concerning the above subject have been carried out and published [11-12]. This review is aimed at giving a general overview of some of the synthetic methods used in the fabrication of nanoparticles.

2. Methods of Synthesis of Nanoparticles

Nanoparticles (NP) can be synthesized either by breaking down the bulk materials into smaller and smaller dimensions or by joining up atoms, molecules or clusters. The former is known as the 'Top down' approach whereas the latter is referred to as the 'Bottom up' method [13].

In the Top-down approach, a block of a bulk material is broken down to get the nanosized particles. Top-down methods of fabrication of nanomaterials include the following, Solid phase techniques namely, Milling (mechanical and mechanochemical), Etching, Electro-explosion, Sputtering, Laser ablation, Lithography, Aresol-based techniques (electrospraying and flame pyrolsis) and Liquid-phase techniques (electrospinning) methods [13]. The main disadvantage of the Top-down approach is the imperfection of the surface structure. For instance, the nanoparticles produced by the attrition have a relatively broad size distribution and various particle shape or geometry. In addition they may contain significant amount of impurities [14-15].

In the Bottom-up approach, the individual atoms and molecules are placed or self assembled precisely where they are needed. Here the molecules or atomic building blocks fit together to produce nanoparticles. Bottom-up approaches are more favorable and popular in the synthesis of nanoparticles and they involve vapor-phase techniques such as Deposition techniques (thermal chemical vapor deposition, plasma-enhanced chemical depositon, and plasma arching), Chemical vapor condensation (molecular beam epitaxy and sputtered plasma processing), Solution-phase techniques (chemical reduction, precipitation, sol- gel, solvothermal synthesis and sonochemical synthesis) and Self assembly techniques (biological templating, electrostatic self-assembly, self assembly monolayers, (SAM) and Langmuir-Blodgett (LB) formation) [13-15].
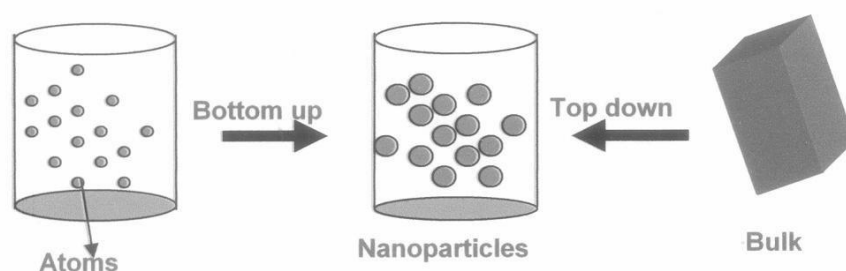
Figure 1: Schematic representation of Bottom–up and Top–down technique

2.1. Mechanical ball milling techniques

Mechanical alloying produces nanostructured materials by the structural disintegration of coarse-grained structures as a result of severe plastic deformation. As a solid state synthetic method, it is usually performed using ball milling equipments that is generally divided into "low energy" and "high energy" category based on the value of the induced mechanical energy to the powder mixture [13, 15]. The synthesis of materials by high energy ball milling of powders was first developed by John Benjamin (1970) and his co-workers at the International Nickel Company in

the late 1960's. The goal of this work was the production of complex Oxide Dispersion-Strengthened (ODS) alloys for high temperature structural applications as well as reduce the particle size and blending of particles in new phases.

Mechanical alloying consists of repeated welding, fracturing and rewelding of powder particles in a dry high-energy ball mill until the composition of the resultant powder corresponds to the percentages of the respective constituents in the initial charge [16]. In this process, mixtures of elemental or pre-alloyed powders are subjected to grinding under a protective atmosphere in equipment capable of high-energy compressive impact forces such as attrition mills, vibrating ball mills and shaker mills. Majority of the works on nanocrystalline materials have been carried out in highly energetic small shaker mills. The process is referred to as mechanical alloying when one starts with a blended mixture of elemental powders and as mechanical milling when one starts with single component powders such as elements or intermetallic compounds. These processes have produced nanocrystalline structures in pure metals, intermetallic compounds and immiscible alloy systems. It has been shown that nanometer-sized grains can be obtained in almost any material after sufficient milling time. The grain sizes are found to decrease with milling time down to a minimum value that appeared to scale inversely with the melting temperature [17-18]. Mechanical ball milling has been used to blend aluminum with magnesium and carbon in order to alter their chemical properties and combustion behavior [19-23]. Several works had been carried out by different researchers on the application of mechanical ball milling to synthesize nanoparticles thus:

For the production of Al- based Nanomaterials and Nano composites, J. Sun *et al* [24] investigated the nanostructural synthesis of the ordered $L1_2+DO22$ multiphase $Al_{67}Mn_8Ti_{24}Nb_1$ alloy by mechanical milling and subsequent annealing. The ordered $L1_2+DO22$ multiphase $Al_{67}Mn_8Ti_{24}Nb_1$ alloy first changed into disordered supersaturated solid solution after 15 h milling and then into the full amorphous structure as the milling continued to about 60 h.

In another development, Manna *et al* [25] reported the synthesis of amorphous and nanocrystalline materials via mechanical alloying of $Al_{65}Cu_{35-x}Zr_x$ (x = 5, 15 and 25at. % Zr) elemental powder by planetary ball milling for up to 50 h. The mechanical alloying of $Al_{65}Cu_{35}$−xZrx (x = 15, 25, 5at.% Zr) by planetary ball milling up to 50h furnished a single-phase amorphous microstructure in $Al_{65}Cu_{20}Zr_{15}$, nanocrystalline and amorphous mixture in $Al_{65}Cu_{10}Zr_{25}$, and nanocrystalline inter-metallic phases in $Al_{65}Cu_{30}Zr_5$, respectively.

Furthermore, nanocrystalline and nano-amorphous $Mg_{1.9}M_{0.1}Ni$ (M_5Ti, Zr, V) alloys were produced by T. Spassov *et al* [26] through mechanical alloying and subsequently by annealing depending on the milling conditions such as rotation speed, duration of milling and annealing (temperature and time of annealing) to give different nanostructures. According to the authors above, the nanomaterials produced possessed hexagonal Mg_2Ni crystal structure as well as the milled and the annealed alloys in the range of 10–20 nm.

 Phase evolution of Fe_2O_3 nanoparticles during high energy ball milling was investigated by Lee *et al* [27]. Here the author employed high-energy ball milling of α-Fe_2O_3 powder in a stainless steel attritor at a speed of 300 rpm for 10 −100 h using a powder-to-ball mass ratio of 1:50 with a powder mass of 100g. Their results revealed that the prolonged milling remarkably reduced particle size from 1 mm in as received powder to about 15 nm in 100 h ball milled powder. Reporting on nano-sized Cu-doped TiO_2 powders using mechanical alloying, Park *et al* [28] stated that nanocrystalline Cu-doped TiO_2 powders were prepared by MM and homogeneous precipitation process at low temperature (HPPLT).

Figure 2: A rock tumbler Ball mills (reprinted from Ref. 20)

2.2. Mechanochemical method

This is the coupling of mechanical and chemical phenomena on a molecular scale and includes mechanical breakage and chemical behavior of mechanically stressed solids *e.g.* stress-corrosion cracking or enhanced oxidation [29]. Mechanochemical synthesis differs from standard ball milling in that, in the standard ball milling process under inert atmosphere results in a moderate reduction of powder particle size and eventually the formation of nanosized grains within micron-sized particles. However, the mechanochemical method involves the initiation of a solid-state displacement reaction during the ball milling process which can result nanosized particles (down to ~5 nm in size) embedded within larger by-product phase particles [30]. The mechanochemical synthesis process has been used in to synthesize a broad range of metal nanoparticles (e.g. Ag, Co, Cr, Cu) etc as well as other compounds such as oxides and sulphides [20, 30]. Disperse particles are formed during mechanochemical synthesis as a result of pulverization of the reagents and chemical interaction between the components. Particles of the reaction products are formed as two- dimensional nuclei at points of contact between reagents; then they grow in volume. Particle size can be controlled by varying the temperature and time of the subsequent heat treatment of the activated mixtures. It has been observed that oxides with particles 1-5 μm in size could be produced through pulverizing, and particles sized 0.02-0.2μm could be obtained by using mechanochemical reactions [31].

However, synthesis by the soft mechanochemical method could give rise to crystalline zirconium titanate formed at 600 ^{o}C [31] according to the reaction given below;

$$Zr(OH)_4 + HTiO_3 \rightarrow ZrTiO + 3H_2O$$
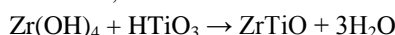
It was also observed that low-temperature mechanochemical treatment could yield a cubic solid solution of ZrO_2-Y_2O_3 in the nanodispersed state [31]. The exchange reaction is shown below;

$$3(ZrO(NO_3)_2 \cdot 2H_2O) + Y_2(CO_3)_3 \cdot 3H_2O \rightarrow (3ZrO_2Y_2O_3) + 3CO_2 + 9H_2O + 6HNO_3$$
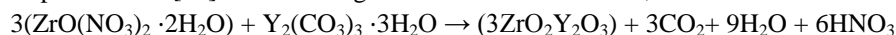
Some examples of sulphides nanoparticles that have been synthesized by mechanochemical process include ZnS, CdS and Ce_2S_3 [32]. It was shown that average particle size of ZnS nanoparticles was reduced when (i) the particle-size of a starting reactant was reduced, (ii) the size of milling media was reduced, or (iii) the volume fraction of ZnS in the product phase was reduced [33]. CdS nanoparticles were synthesised using the reaction.

$$Na_2S + CdCl_2 + 15.6 \, NaCl \rightarrow CdS + 17.6 \, NaCl \, [34].$$
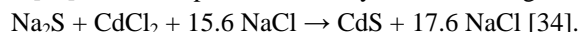
The authors [32-35] maintained that it was possible to control mean particle sizes from 4 to 8 nm by varying the size of grinding media and after milling for 4 hours with milling media of 4.8 mm in diameter and subsequent washing to remove NaCl, CdS nanoparticles of ~4 nmin diameter were obtained [35]. Various oxides nanoparticles have been synthesized via mechanochemical methods. The reactions below are some examples of mechanochemical reactions showing different oxide nanoparticles that have been synthesized by mechanochemical method [32-35].

$$2AlCl_3 + CaO \rightarrow Al_2O_3 + 3CaCl_2$$
$$ZrCl_4 + 2CaO \rightarrow ZrO_2 + 2CaCl_2$$
$$GdCl_3 + 3NaOH \rightarrow Gd_2O_3 + 3NaCl + 1.5H_2O$$
$$CeCl_3 + NaOH \rightarrow CeO_2 + 3NaCl + H_2O$$
$$Na_2Cr_2O_7 + S \rightarrow Cr_2O_3 + Na_2SO_4$$
$$2NbCl_5 + 5Na_2CO_3 \rightarrow Nb_2O_5 + 10NaCl + 5CO_2$$
$$SnCl_2 + Na_2CO_3 + O_2 \rightarrow SnO_2 + 2NaCl + CO_2$$
$$2FeCl_3 + 3Ca(OH)_2 \rightarrow Fe_2O_3 + 3CaCl_2 + 3H_2O$$
$$ZnCl_2 + Na_2CO_3 \rightarrow ZnO + 2NaCl + CO_2$$
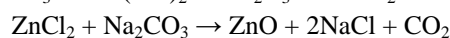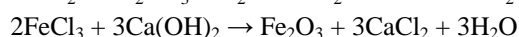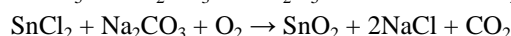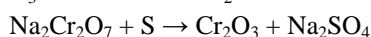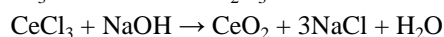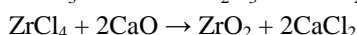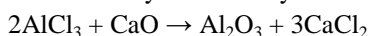
2.3. Etching Techniques

This is traditionally the process of using strong acid or mordant (a corrosive liquid) to cut into the unprotected parts of a metal surface to create a design in the metal. In the modern approach of micro fabrication, different etching methods are used and these are the wet chemical etching and dry etching [36].

Wet etching

Wet etching is a material removal process that uses liquid chemicals or etchants to remove materials from a wafer. The specific patterns are defined by masks on the wafer. Materials that are not protected by the masks are etched

away by liquid chemicals. These masks are deposited and patterned on the wafers in a prior fabrication step using lithography. This method requires a container with a liquid solution that will dissolve the material in question. Unfortunately, there are complications since usually a mask is desired to selectively etch the material. One must find a mask that will not dissolve or at least etches much slower than the material to be patterned. Secondly, some single crystal materials, such as silicon, [36] exhibit anisotropic etching in certain chemicals. Anisotropic etching in contrast to isotropic etching means different etches rates in different directions in the material. The wet method is used in the production of silicon wafer in a chemical such as potassium hydroxide (KOH). Marwa and Hussien [37] reported the preparation of silica nanoparticles by w*et al*kali chemical etching technique of commercial silicon powder using (KOH, n-propanol and water). They dispersed an appropriate amount of Si-powder in a solution containing potassium hydroxide (KOH), n-propane and distilled water and the mixture was milled for about 20 minutes and the gray color Si-powder was turned to brown after the etching was finished.

In another development, Wei Cheng *et al* [38] also reported an etching method that was used to synthesize nanosized iron oxide with small primary particle sizes of approximately 4 nm and a high specific surface area of 317 $m^2\,g^{-1}$. This material was used as an adsorbent for arsenic removal from water as shown below;
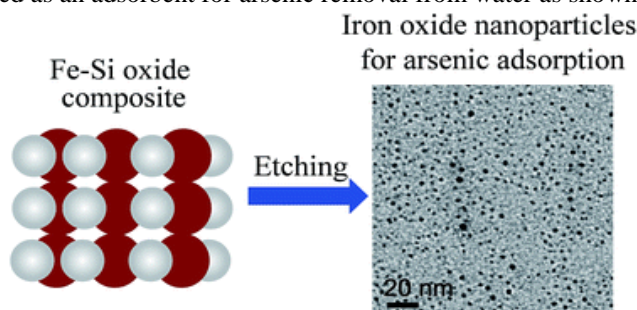
Figure 3: An etching method used to synthesize nanosized iron oxide.

Kwangjin *et al* [39] synthesized various hollow oxide nanoparticles from as-prepared MnO and iron oxide nanocrystals by heating metal oxide nanocrystals dispersed in technical grade trioctylphosphine oxide (TOPO) at 300 °C for hours which retained the size and shape uniformity of the original nanocrystals. The authors maintained that this method is highly reproducible and could be generalized to synthesize hollow oxide nanoparticles of various sizes, shapes, and compositions. They also claimed that the impurities present in technical grade TOPO, especially alkylphosphonic acid during the experiment, were responsible for the etching of metal oxide nanocrystals to the hollow structures.

Dry etching
Dry etching refers to the removal of material, typically a masked pattern of semiconductor material, by exposing the material to a bombardment of ions (usually a plasma of reactive gases such as fluorocarbons, oxygen, chlorine, boron trichloride; sometimes with addition of nitrogen, argon, helium and other gases) that dislodge portions of the material from the exposed surface. A common type of dry etching is reactive-ion etching. Dry etching technology can be split in three separate classes called reactive ion etching (RIE), sputter etching, and vapor phase etching. In RIE, the substrate is placed inside a reactor in which several gases are introduced. Plasma is produced in the gas mixture by using a radio frequency (RF) power source to break the gas molecules into ions. The cations produced from reactive gases are accelerated with high energy to the substrate and chemically react with the silicon. The typical RIE gasses for Si are CF_4, SF_6 and $BCl_2 + Cl_2$ [36]. This is known as the chemical part of reactive ion etching.

Physical dry etching requires high energy (ion, electron, or photon) beams to etch off the substrate atoms. When the high energy particles knock out the atoms from the substrate surface, the material evaporates after leaving the substrate. There is no chemical reaction taking place and therefore only the material that is unmasked will be removed. [40]. A schematic of a typical reactive ion etching system is shown in the figure 4.0 below.
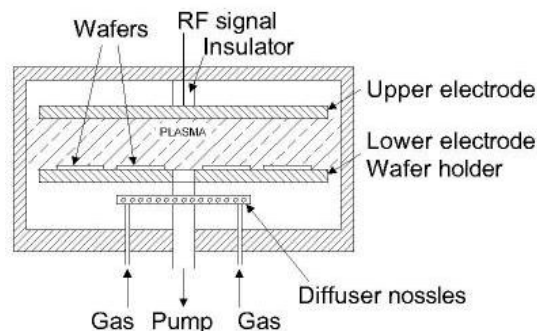
Figure 4: A typical reactive ion etching system

Sputter etching is essentially RIE without reactive ions. The operations used are very similar in principle to sputtering deposition systems. The big difference is that substrate is now subjected to the ion bombardment instead of the material target used in sputter deposition [36, 40].

A new method to form metal nanoparticles by sputter deposition inside a reactive ion etching chamber with a very short target-substrate distance was reported by Min *et al* [40]. According to these authors, the distribution and morphology of nanoparticles were found to be affected by the distance, the ion concentration, and the sputtering time. Densely distributed nanoparticles of various compositions were fabricated on the substrates that were kept at a distance of 130 μm or smaller from the target. When the distance was increased to 510 μm, island structures were formed, indicating the tendency to form continuous thin film with longer distance. The primary target used was a 15x15 mm^2 brass foil alloy 260, Cu : Zn=70:30, with parallel openings of 50x1000 m^2 patterned by laser cutting. For comparison, other targets consisting of Cu, Al, and Cr were employed and several nanomaterials of these metals were reported to be deposited by this technique.

Vapor phase etching is another dry etching method, which can be done with simpler equipment than what RIE requires. Chemical dry etching (also called vapor phase etching) does not use liquid chemicals or etchants. In this process the wafer to be etched is placed inside a chamber, in which one or more gases are introduced. The process involves a chemical reaction between etchant gases to attack the silicon surface. The material to be etched is dissolved at the surface in a chemical reaction with the gas molecules. The two most common vapor phase etching technologies are silicon dioxide etching using hydrogen fluoride (HF) and silicon etching using xenon diflouride (XeF$_2$), both of which are isotropic in nature. Usually, care must be taken in the design of a vapor phase process so as to avoid the formation of bye-products in the chemical reaction that condense on the surface and interfere with the etching process [41].

Nearly all silicon MEMS (Micro Electro Mechanical Systems) [42] devices are produced by using a sacrificial silicon oxide layer, which when removed, "releases" the silicon MEMS structure and allows free movement. Silicon oxide is typically etched by hydrogen fluoride as shown in the chemical reaction below;

$$SiO_2 + 4HF \rightarrow SiF_4 (g) + 2H_2O$$

The most widespread method of HF [41, 42] based etch release is wet chemical etching using a mixture of HF and water. However, as the HF, or the accessory rinsing solutions, dries, it can cause "stiction"; by pulling the free-moving micro-materials produced together which remain adhered to each other after release, thereby reducing the yield. Another problem with wet HF etching is that it corrodes any exposed metals, especially aluminium, on the wafer.

Therefore in order to avoid all the above shortcomings, dry HF becomes the best alternative [41, 42]. The reason is that a gaseous etchant penetrates smaller features more easily and allows longer undercuts. In this method, an alcohol (A) is used to ionize the HF vapor and acts as a catalyst:

$$SiO_2(s) + 2HF_2^-(ads) + 2AH^+ (ads) \rightarrow SiF_4(ads) + 2H_2O (ads) + 2A (ads)$$
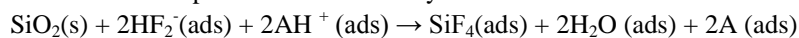
The by-product of the reaction (water), also acts as a catalyst but must be carefully controlled and removed from the system [41, 42].

2.4. Sputtering

This is a process whereby particles are ejected from a solid target material due to bombardment of the target by energetic particles [43] particularly, in the laboratory as gas ions. This can happens when the kinetic energy of the incoming particles is much higher than conventional thermal energies. Instead of using heat to eject material from a source, they can be bombarded with high speed particles. The momentum transfer from the particles to the surface atoms can impart enough energy to allow the surface atoms to escape. Once ejected, these atoms (or molecules) can travel to a substrate and deposit as a film. So in sputtering, the target material and the substrate are placed in a vacuum chamber. A voltage is applied between them so that the target is the cathode and the substrate is attached to the anode [43]. Plasma is created by ionizing a sputtering gas (generally a chemically inert, heavy gas like Argon). The sputtering gas bombards the target and sputters off the material of interest to be deposited.

Sporn et al in 1997 [44] and Thompson in 1966 [45] employed the sputtering techniques to synthesis silicon and gold nanoparticles respectively.

Sputtering observed to occur below the threshold energy of physical sputtering is also often called chemical sputtering [43-45] but the mechanisms behind such sputtering are not always well understood, and may be hard to distinguish from chemical etching. At elevated temperatures, chemical sputtering of carbon can be understood to be due to the incoming ions weakening bonds in the sample, which then desorbs by thermal activation [46]. The hydrogen-induced sputtering of carbon-based materials observed at low temperatures has been explained by H ions entering between C-C bonds and thus breaking them [41].

Perekrestov *et al* [47] investigated on TiO_2 nanoparticles synthesis and reported that, these Nanoparticles were obtained in Argon plasma on monocrystaline Si (111) substrate by gas-phase deposition technique using hollow cathode plasma jet (HCPJ). A pure material of titanium was used as the cathode whose surface had a very high affinity for oxygen and thus facilitating the formation of a layer of oxide when exposed to the atmosphere or by the introduction of oxygen into the main chamber. This method is based on sputtering $TiO_2/Ti_2O_3/TiO$ layer of a hollow cathode. The authors gave explanation of nanoparticle growth mechanism and size distribution, morphology of thin film surface by means of scanning electron microscope (SEM) and atomic force microscope (AFM), while mass spectrometer was used to monitor the chemical composition of the gas inside the system during deposition. The chemical composition of the thin films was investigated by means of energy-dispersive x-ray analysis (EDX).

2.5. Laser ablation

Laser ablation refers the removal of material from a surface using laser irradiation. A typical schematic diagram of laser ablation is shown in the following figure [48].
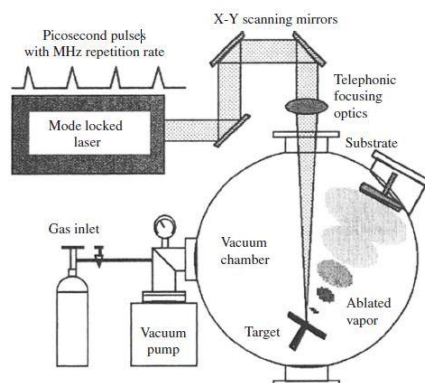
Figure 5: A typical schematic diagram of laser ablation

The laser ablation device consists of two essential parts, namely a pulsed laser and an ablation chamber [48]. The high power of the laser beam induces large light absorption on the surface of target, which makes temperature of the absorbing material increase rapidly. As a result, the material on the surface of target vaporizes into laser plume [49]. In some cases, the vaporized materials condensate into cluster and particle without any chemical reaction. In some other cases, the vaporized material reacts with introduced reactants to form new materials. The condensed particles

will be either deposited on a substrate or collected through a filter system consisting of a glass fiber mesh. Then, the collected nanoparticles can be coated on a substrate through drop-coating or screen-printing process [49-50]

Pulsed laser synthesis (PLS) is a powerful, flexible and versatile technique in the synthesis of many nanoparticles without employing special external conditions, such as high pressure or high temperature. It is flexible in that it can be integrated with other techniques such as chemical vapor deposition [51]. In addition, it can be used to synthesize various nanostructures via different experimental setups as well as to fabricate the same nano structures by different approaches, making it a versatile technique. PLA is used in the top-down synthesis of nanomaterials, such as nanotubes [52], nanowires [53], nano-ribbons [54], quantum dots [55, 56], and even nano-flakes of the material. The technique is widely used by many researchers in the synthesis of both inorganic and carbon-based materials with varying particle sizes and in high yield as well as aluminum nanoparticles [57, 58]. PLA was first reported by Patil *et al*. in 1987 [59], forming iron oxides with metastable phases by PLA of a pure iron target placed in water.

Williams and Coles [60, 61] prepared nanocrystalline SnO_2 by a laser ablation technique for detection of CO, H_2, and CH_4. Their studies revealed that the gaseous atmosphere in which the condensation of the laser-ablated SnO_2 occurs has a significant influence on the size of the nanoparticles generated. The use of Ar at the pressure of 1 bar to replace the standard conditions employed in air at 1 bar led to a decrease in SnO_2 grain size to 8 nm. Furthermore, by shortening the laser pulse from the customary 20 ms to 30 ns employing a XeCl excimer laser, a further reduction in the grain size was achieved. Their gas sensors based on nanocrystalline SnO_2 powders prepared by laser ablation and gas-phase condensation route offered enhanced sensitivity to CO, H_2, and CH_4 compared with the materials prepared by conventional methods.

Hu and his co-workers prepared nanocrystalline SnO_2 thin film using a SnO_2 target and a metallic Sn target respectively for C_2H_5OH detection [48]. Their results demonstrated that the oxidation of Sn into SnO_2 depends strongly on the substrate temperature. Oxidation of Sn into SnO_2 proceeds mainly on the substrate surface instead of in the ablation plume during the condensation of Sn species onto the substrate, even if the ambient oxygen pressure reaches 100–150 Pa.

Starke and Coles [62] reported their gas sensors prepared using laser ablated nanocrystalline metal oxides. They found that SnO_2 and In_2O_3 are capable of detecting ozone at concentrations well below 100 ppb with response times of less than one minute. Pt doped SnO_2 and, particularly, In_2O_3 show some cross sensitivity to NO and NO_2. WO_3 shows sensing properties superior to these two materials in terms of selectivity and response time but regrettably does not exhibit such high sensitivity. Their CO sensor is highly sensitive to single-figure ppm concentration with a resolution down to 1 ppm. These studies demonstrate that the laser ablated nanostructured metal oxides can greatly enhance the sensing performance of gas sensors.

2.6. Inert gas Condensation

The inert gas evaporation–condensation (IGC) technique, in which nanoparticles are formed via the evaporation of a metallic source in an inert gas, has been widely used in the synthesis of ultrafine metal particles since the 1930s [63]. This technique is used to synthesize small quantities of nanostructured pure metals. It involves evaporation of metal using any of these heating sources, resistive heating, radiofrequency heating, sputtering, electron beam heating, laser/plasma heating, or ion sputtering, inside a chamber that has been evacuated to a very high vacuum of about 10^{-7} torr and then backfilled with a low pressure inert gas like helium [64]. The evaporated atoms collide with the gas atoms inside the chamber, lose their kinetic energy and condense in the form of small, discrete crystals of loose powder. Convection currents, generated due to the heating of the inert gas by the evaporation source and cooled by the liquid nitrogen-filled collection device (cold finger), carry the condensed fine powders [64, 65] to the collector device, from where they can be stripped off by a scrapper in the form of a metallic plate.

The crystal size of the powder obtained depends upon the inert gas pressure, the evaporation rate and the gas composition. It is typically a few nanometers and the size distribution is narrow. However, extremely fine particles can be produced by decreasing either the gas pressure in the chamber or the evaporation rate and by using light inert gasses (such as He) rather than heavy inert gases (such as Xe) [64]. Reports on the results obtained from

experiments using the inert gas condensation method to produce nanoparticles of Mn, AuPd and CoO, Y_2O_3 have been in literature [65, 66].
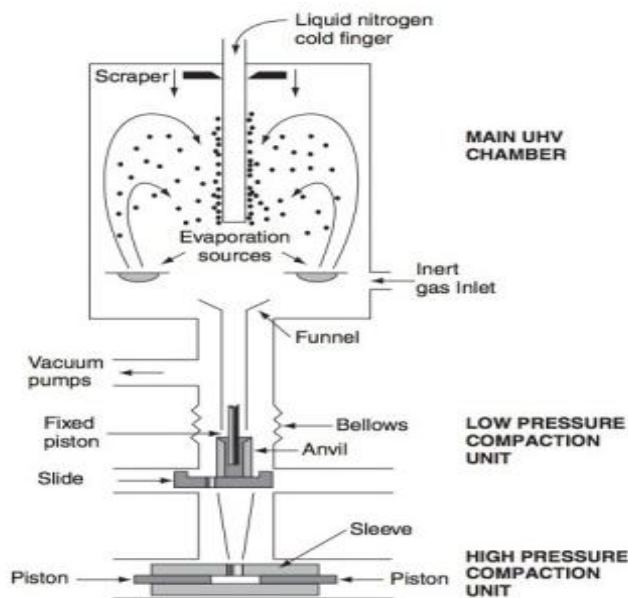
Figure 6: Schematic diagram of inert gas condensation method

Wesley *et al* [67] also reported on the preparation conditions adopted to obtain different morphologies of as-deposited refractory metal-oxide (Y_2O_3) nanoparticles using inert-gas condensation with CO_2 laser heating. According to them, the micrometer-scale morphology of the nanoparticles obtained depended on the specific metal oxide, the buffer gas composition and pressure as well as the target-to-substrate distance. The above parameters actually controlled and determined the extent to which a plume of nonagglomerated nanoparticles reached the deposition substrate. They also maintained that the buffer gas pressure used offered the largest influence for a given material, with lower pressures producing a dense columnar morphology and higher pressures resulting in an open networked morphology. They concluded that an estimate based on the geometry of the gas-phase plume and experimental results for Y_2O_3 nanoparticles produced in 4 Torr N_2 gave a critical concentration of tens of nanoparticles per μm^3 for the transition of agglomerates versus isolated nanoparticles reaching a deposition substrate.

Ward *et al* [68] presented their reported from experiments carried out using the inert gas condensation method to produce manganese nanoparticles which included both Mn_3O_4 and pure Mn particles. The authors claimed that the use of moisture in untreated helium gas caused the particles to oxidize, whereas when the helium was run through liquid nitrogen, it trapped and removed the moisture thereby producing $\beta-$Mn particles in a metastable state. The particle sizes and the size distribution were determined to range from 2 nm to above 100 nm.

2.7. Chemical Vapor Synthesis

There are two major methods that make up the Chemical Vapor Synthesis approach and these are (a) chemical vapor condensation (CVC) and (b) Chemical Vapor deposition (CVD)**.** They have tremendous flexibility in producing a wide range of materials and can take advantage of the huge database of precursor chemistries that have been developed for the production of nanoparticles.

(a) Chemical vapor condensation (CVC)

In chemical vapor condensation, vapor phase components are brought into a hot-wall reactor under conditions that favor nucleation of particles in the vapor phase rather than deposition of a film on the wall which occurs in Chemical Vapor deposition (CVD)**.** The precursors can be solid, liquid or gas at ambient conditions, but are

delivered to the reactor as a vapor (from a bubbler or sublimation source, as necessary) [48]. Chemical Vapor Condensation (CVC) process was developed in Germany in 1994 [69].

When a mixture of gas reactants are delivered into a reaction chamber, the chemical reactions among the gas molecules are induced by an input of energy such as resistant heating, laser, and plasma. Chlorides are the popular reactants for the formation of oxides because of their generally low vaporization temperature and low cost. A typical reaction is represented below [48]:

$$SnCl_{4\,(g)} + 2H_2O_{\,(g)} \rightarrow SnO_{2\,(s)} + 4HCl_{\,(g)}$$
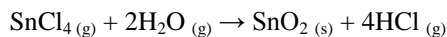
Another key feature of chemical vapor synthesis is that it allows formation of doped or multi-component nanoparticles by use of multiple precursors. Schmechel *et al* [70] prepared nanocrystalline europium doped yttria (Y_2O_3:Eu^{3+}) from organometallic yttrium and europium precursors. Senter *et al* [71] incorporated erbium into silicon nanoparticles using disilane and an organometallic erbium compound as precursors. Brehm *et al* [72] synthesized doped nanoparticles of zinc oxide by chemical vapor synthesis for the applications as transparent conducting oxides, catalysts and gas sensors. The dopant elements, aluminum, gallium, and indium influence the particle size of the powders as well as lattice parameters and local structure. The powders exhibit a narrow size distribution with an average size of about 5 nm.
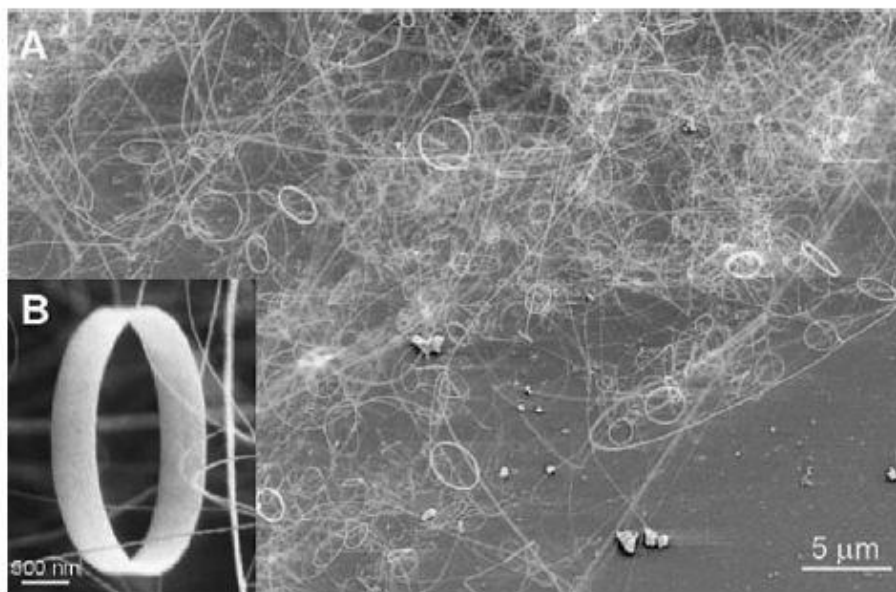
Figure 7: (A) Low-magnification SEM image of the as-synthesized ZnO nanorings. (B) High magnification SEM image of a freestanding single-crystal ZnO nanoring, showing uniform and perfect geometrical shape. The ring diameter is 1 to 4 µm, the thickness of the ring is 10 to 30 nm, and the width of the ring shell is 0.2 to 1 µm. (After ref. 48).These metal oxide nanobelts, nanowires, nanodiskettes, and nanoribbons are highly promising candidates for gas sensing materials. Other Nanoparticles that have been synthesized by include ZrO₂, Y₂O₃ [77-78].

Wang's group [73-76] successfully synthesized a series of binary semiconducting oxide nanobelts (or nanoribbons), such as ZnO, In_2O_3, $Ga_2\,O_3$, CdO and PbO_2 and SnO_2 by simply evaporating the source compound. Condensed or powder source materials were vaporized in a tube furnace at an elevated temperature and the resultant vapor phase condense under certain conditions (temperature, pressure, substrate, etc.) to form the desired products. The as synthesized oxide nanobelts are pure, structurally uniform, single crystalline and most of them free from defects and dislocations with a rectangular-like cross-section with typical widths of 30 to 300 nanometers, width-to-thickness ratios of 5 to 10, and lengths of up to a few millimeters. The belt-like morphology appears to be a unique and common structural characteristic for the family of semiconducting oxides with cations of different valence states and materials of distinct crystallographic structures. The nanobelts are an ideal system for fully understanding

dimensionally confined transport phenomena in functional oxides and building functional devices along individual nanobelts. The above authors [72-75] have applied the nanobelt materials to make the world's first field effect transistor and single wire sensors. The latest breakthrough of Wang's group is the success of first piezoelectric nanobelts and nanorings [75] for applications as sensors, transducers and actuators in micro and nano-electromechanical systems. A typical SEM image of as-synthesized ZnO nanorings is shown in the following figure. Owing to the positive and negative ionic charges on the zinc- and oxygen-terminated ZnO basal planes, respectively, a spontaneous polarization normal to the nanobelt surface is induced. As a result, helical nanosprings/nanocoils are formed by rolling up single crystalline nanobelts. The mechanism for the helical growth is suggested for the first time to be a consequence of minimizing the total energy contributed by spontaneous polarization and elasticity. The nanobelts have widths of 10–60 nanometers and thickness of 5–20 nanometers, and they are free of dislocations. The polar surface dominated ZnO nanobelts and helical nanosprings are likely to be an ideal system for understanding piezoelectricity and polarization induced ferroelectricity at nano-scale.

(b) Chemical Vapor Deposition (CVD)

$$[Me_3GA]_{(g)} + [AsH_3]_{(g)} \xrightarrow{500^oC-700^oC} GaAS_{(s)} + 3CH_{4(g)} \uparrow$$

$$[SiH_4]_{(g)} \xrightarrow{500^oC-800^oC} Si_{(s)} + 2H_{2(g)} \uparrow$$

$$[SiH_4]_{(g)} + O_{2(g)} \xrightarrow{350^oC-475^oC} SiO_{2(s)} + 2H_{2(g)} \uparrow$$

$$2[Ta(OEt)_5]_{(v)} + 5H_2O_{(v)} \xrightarrow{350^oC-475^oC} Ta_2O_5 + 10EtOH_{(v)} \uparrow$$

$$[NbCl_5]_{(v)} + {}^5/_2H_2O(g) + {}^1/_2xN_2(g) \xrightarrow{900^oC} NbNx + 5HCl_{(v)} \uparrow$$
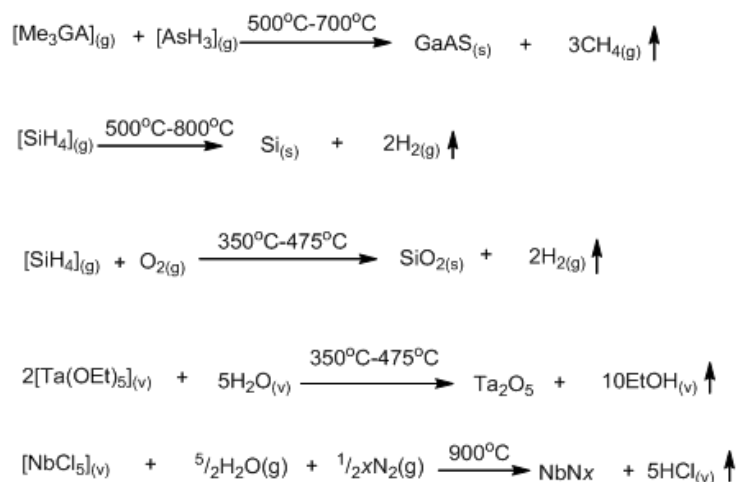
Overall reaction schemes for a variety of CVD processes.

Chemical Vapor Deposition (CVD) is a process in which a thin solid film is deposited on a heated surface via a chemical reaction from the vapor or gas phase. There are different types CVDs and they include thermal CVD, plasma CVD D, laser CVD, photo-laser CVD, metal-organic chemical vapor deposition (MOCVD) etc [69]. In thermal CVD, the reaction is activated by a high temperature above 900°C. A typical apparatus comprises of a gas supply system, a deposition chamber and an exhaust system. In plasma CVD, the reaction is activated by plasma at temperatures between 300 and 700 °C [69]. In laser CVD, pyrolysis (decomposition brought about by high temperatures) occurs when laser thermal energy heats an absorbing substrate. In photo-laser CVD, the chemical reaction is induced by ultra violet radiation which has sufficient photon energy to break the chemical bond in the reactant molecules. In this process, the reaction is photon activated and deposition occurs at room temperature.

CVD processes are extremely complex and involve a series of gas-phase and surface reactions. They are often summarized by overall reaction schemes listed below [79, 80].

A more detailed picture of the basic physicochemical steps in an overall CVD reaction is illustrated in Figure below and it involves four (4) steps [80].

1. Evaporation and transport of precursors in the bulk gas flow region into the reactor;
2. Gas phase reactions of precursors in the reaction zone to produce reactive intermediates and gaseous by-products;
3. Mass transport of reactants to the substrate surface;
4. Adsorption of the reactants on the substrate surface;
5. Surface diffusion to growth sites, nucleation and surface chemical reactions leading to film formation;

6. Desorption and mass transport of remaining fragments of the decomposition away from the reaction zone.
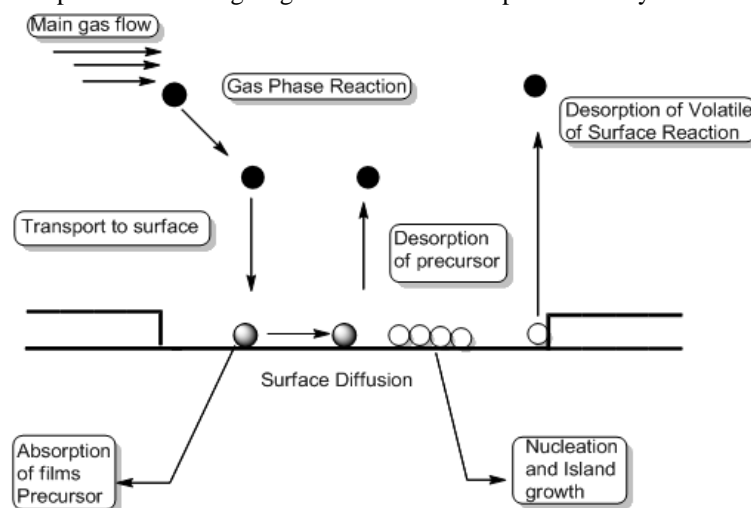
Figure 8: Precursor transport and reaction processes in CVD

Jing *et al* [79] reported the synthesis of high quality single-walled carbon nanotubes (SWNT) by chemical vapor deposition (CVD) of methane at 1000^oC on supported Fe_2O_3 catalysts. This type of catalyst support was found to control the formation of individual bundled SWNTs. The authors highlighted that the catalysts supported on crystalline alumina nanoparticles produced abundant individual SWNTs and small bundles while those supported by amorphous silica particles produce only SWNT bundles. Their studies of the ends of SWNTs led to an understanding of their growth mechanism. They also investigated on the use of methane CVD on supported NiO, CoO and NiO/CoO catalysts. From their investigation, they reported that none of the NiO/alumina and NiO/silica catalysts produced SWNTs while CoO and NiO/CoO catalysts produced SWNTs only on one of the alumina or silica supports.

Pavel *et al* [82] reported the synthesis of Ni/NiO nanoparticles by using metal organics chemical vapor deposition of nickel acetylacetonate in an externally heated tube flow reactor at moderate temperatures, up to 500 ^{o}C. The author studied the particles production and characteristics by evaluating the effects of reactor temperature, precursor concentration, and flow rate through the reactor. Che *et al* [83] developed a new approach for preparing graphitic carbon nanofiber and nanotube ensembles via chemical vapor deposition (CVD) synthesis of carbon within the pores of an alumina template membrane with or without a Ni catalyst. The authors used ethylene or pyrene in the above process with reactor temperatures of 545 °C for Ni-catalyzed CVD and 900 °C for the uncatalyzed process. The result obtained from their studies revealed that the resultant carbon nanostructures produced were uniform hollow tubes with open ends. They claimed that by increasing the deposition time the carbon nanotubes were converted into carbon nanofibers.

2.8. Electrochemical deposition of nanomaterials

Electrochemical deposition is a deposition process in which metal ions in a solution are transported by an electric field to coat the surface of a substrate. The deposition process can be either cathodic or anodic reaction depending on the work piece to be coated (cathode or anode), the metallic ions are attracted to the cathode and reduced to metallic form. The diagram below illustrate the above process where (1) is the material to be deposited (anode) (2) the deposited metal (nanoparticles) on the cathode (3) the metallic ions [84].

Electrodeposition of nanostructures, eg. nanocrystallines, nanocomposites, amorphous film or layered materials can be obtained by controlling the electrolysis parameters [84, 85]. The most commonly practiced techniques are (a) pulse current deposition to manipulate the growth of deposits, (b) deployment of additives and surfactants to alter the grain size of deposits and (c) nanoparticles inclusion into deposits to form nanocomposites [84].
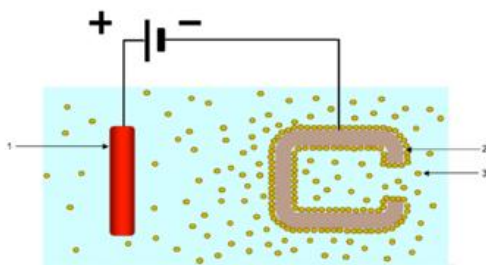
Figure 9: Electrochemical deposition is a deposition

(a) Pulse current electrodeposition of nanostructured coating
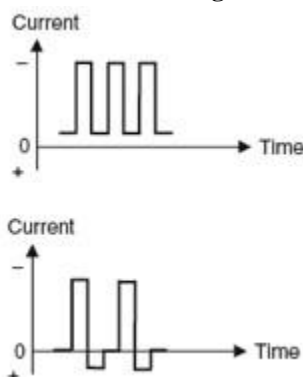
Figure 10

Direct current is the most commonly deployed technique to deposit a metal coating. Recent years have seen the use of pulsating the current to achieve nanostructure coating. The pulse regime parameters include pulse duty, pulse cycle, frequency and its amplitude, cathodic or anodic current, zero current at open-circuit etc [84-86]. Pulsating the deposition current can affects the diffusion layer next to the electrode surface which is in contact with the liquid solution. This will influence the deposition mechanisms of metal deposits such as altering the nucleation process and the subsequent growth of the deposit. Pulsed current can enable the incorporation of nanoparticles to a high content in the coating as well as producing a wider range of alloys, deposit composition and material properties [86].

(b) Nanoparticles in a metal coating to form nanocomposites

Nanosized particles can be incorporated into metallic coating to form nanocomposite coating [86, 87].
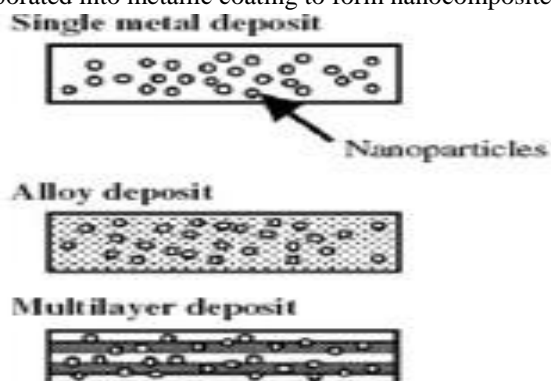
Figure 11

Two common processes involved in the incorporation of particles into metallic coatings are (a) physical dispersion of particles in the electrolyte and (b) electrophoresis migration of particles to the work piece supported by surface charged particles. The metal coating can be plain metal, eg. nickel, silver, copper, tin, gold, or alloys and

multilayered coatings [88]. Nanoparticles may include metals, alloys, ceramics, metal oxides, nitrides, carbides, etc [85, 86]. The inclusion of nanoparticles into a metal coating is dependent on many electrolysis parameters such as characteristics of the nanoparticle (particle concentration, surface charge, type, shape, size), electrolyte composition (electrolyte concentration, additives, temperature, pH, surfactant type and concentration), current density (direct current, pulsed current, potentiostatic control) and flow hydrodynamics (laminar, turbulent regimes), electrode geometry and electrodeposition reactor, e.g. rotating disk electrode, rotating cylinder electrode, parallel plate electrodes, etc. Figures below show electrodeposited nickel coatings containing nanoparticles of silicon carbide (SiC) and titanium dioxide nanotubes (TiO_2), for wear and corrosion resistance [89, 90].
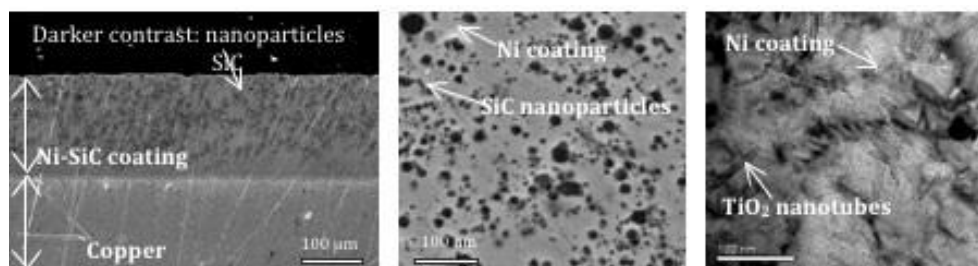
Figure 12

(c) Deployment of electrolyte additives and surfactant technology

Electrolyte additives and surfactant technology are keys to the development of nanostructured materials and coatings [93]. Surfactants can be categorized into groups such as: cationic, anionic, non-ionic or amphoteric [94]. Surfactants can be hydrocarbon or fluorocarbon based [95]. In the surface metal finishing industry, electrolyte additives are commonly grouped by names such as brighteners (provide surface finish as matte, semi-matte or bright appearance), surface wetters (reduce surface tension between, reduce coating porosity or liberation of gas bubbles) and stress relievers (relieve compressive or tensile stress of the coating). Additives and surfactants are deployed to affect the growth of metal deposits, via adsorption or desorption mechanisms [96].

Many metallic coatings are conventionally designed on the macro-scale. By reducing the macro-scale to the nano-scale could provide enhanced surface properties, leading to a longer lasting, lighter weight and more protective coatings. Electrolyte additives and surfactants are used to affect the grain size of coating [94, 95, and 96]. The figure shows a polycrystalline *vs.* nanocrystalline coating. A nanocrystalline coating has nm grain size, with enhanced coating performance against an external load.
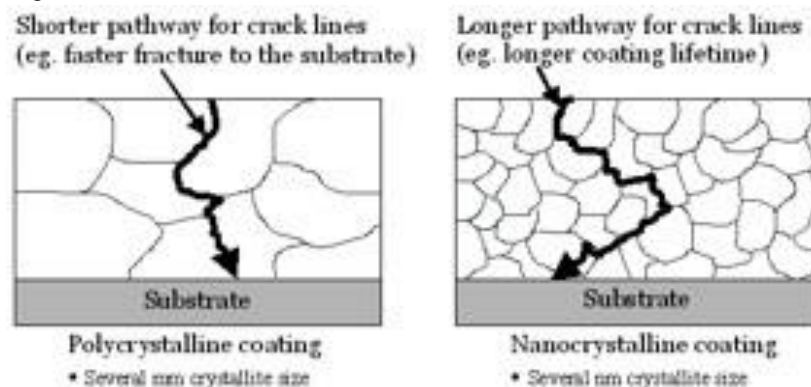
Figure 13

Crystalline maghemite (γ-Fe_2O_3) nanoparticles cathodically electrodeposited at room temperature from environmentally benign electrolytes was studied by Park *et al* in 2008 [87]. The shape, size, and production rate of nanoparticles were strongly influenced by electrochemical conditions (e.g. $FeCl_3$ concentration, current density). Mohanty [85] reported the synthesis of various nanoscale materials, such as nanoparticles, nanowires of Au, Pt, Ni Co, Fe, Ag etc., by electrodeposition techniques. The author employed two different methods namely, potentiostatic

and galvanostatic methods to carry out the electrodeposition process under different potential ranges, time durations, and current densities. He also investigated on the electrochemical behavior of the deposited nanoparticles on various substrates by cyclic voltammetric and chronoamperometric techniques. He also highlighted on the synthesis of mono-dispersed gold (Au) nanoparticles on indium tin oxide (ITO) coated glass, preparation of Au nanorods on nanoporous anodic alumina oxide (AAO), formation of Au nanoclusters on polypyrrole-modified glassy carbon electrode and one-step electrodeposition of nickel nanoparticle chains embedded in TiO_2 etc. in his studies.

2.9. Chemical Precipitation

A precipitate is a solid that forms out of solution. A common example is that of the mixing of two clear solutions *e.g.* silver nitrate ($AgNO_3$) and sodium chloride (NaCl). The reaction is shown as;

$$AgNO_{3(aq)} + NaCl_{(aq)} \longrightarrow NaNO_{3(aq)} + AgCl_{(aq)}$$
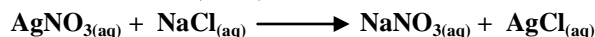
A chemical precipitation process consists of three main steps: chemical reaction, nucleation and crystal growth. Chemical precipitation is generally not a controlled process in terms of reaction kinetics and the solid phase nucleation and growth processes. Therefore, solids obtained by chemical precipitation have a wide particle size distribution plus uncontrolled particle morphology, along with agglomeration [97]. In this strategy the size is controlled by arrested precipitation technique. Thus this is achieved by basic synthesizing and studying the nanomaterial in situ i.e. in the same liquid medium avoiding the physical changes and aggregation of tiny crystallites. Thermal coagulation and Oswald ripening are controlled by double layer repulsion of crystallites using non-aqueous solvents at lower temperatures for synthesis [97]. The synthesis involved reaction between constituent materials in suitable solvent. The dopent is added to the parent solution before precipitation reaction while a surfactant is used to maintain separation between the particles formed [93, 94]. Thus formed nanocrystals are separated by centrifugation, washed and vacuum dried. The dried material was further subjected to UV curing for possible polymerization of surfactant capping film on the surface of nano-clusters for imparting true quantum confinement [95, 96].

Bahari *et al* [98] successfully prepared NiO nanopowder by chemical precipitation method, using nickel nitrate hex hydrate and sodium hydroxide as raw materials. The majority of obtained NiO nanopowders had an average particle size less than 50nm in all cases. The main materials used were nickel nitrate hexa hydrate ($Ni(NO_3)_2 \cdot 6H_2O$), sodium hydroxide (NaOH), polyvinilpyrolidone (PVP, MW = 65000), polyethylene glycol (PEG, MW = 15000), and cetyl trimethyl ammonium bromide (CTAB). Main reactions occur during the experimental procedure can be written briefly as follows:

$$2\ NaOH_{(s)} \longrightarrow 2\ Na^+_{(aq)} + 2OH^-_{(aq)}$$

$$Ni(NO_3)_2 \cdot 6H_2O_{(s)} \longrightarrow Ni^{2+}_{(aq)} + 2\ NO_3^-(aq) + 6H_2O_{(l)}$$

$$Ni^{2+}_{(aq)} + 2\ OH^-_{(aq)} + x\ H_2O_{(aq)} \longrightarrow Ni(OH)_2 \cdot x\ H_2O_{(s)} \downarrow$$

$$Ni(OH)_2 \cdot x\ H_2O_{(s)} \xrightarrow{50\ -\ 100^oC} Ni(OH)_{2(s)} + x\ H_2O_{(g)}$$

$$Ni(OH)_{2(s)} \longrightarrow NiO_{(s)} + H_2O_{(g)}$$
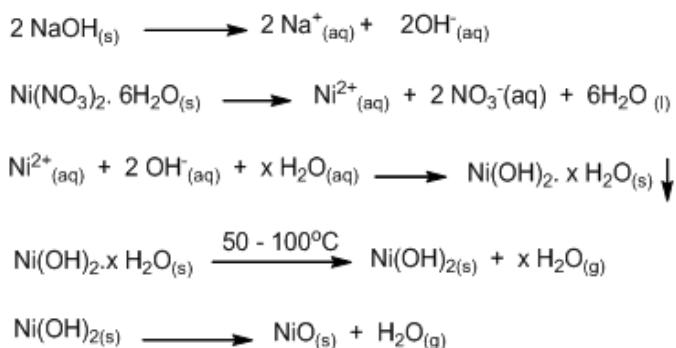
Hamid *et al* [99] synthesized ZnO nanoparticles by direct precipitation method using zinc nitrate and KOH as precursors. The authors used (0.2M) aqueous solution of zinc nitrate ($Zn\ (NO_3)_2 \cdot 6H_2O$) and (0.4 M) KOH solution in the presence of deionized water, respectively. The procedure adopted by the authors is given thus; KOH solution was slowly added into zinc nitrate solution at room temperature under vigorous stirring, which resulted in the formation of a white suspension. The white product obtained was then centrifuged at 5000 rpm for 20 min and washed three times with distilled water, finally with absolute alcohol. The obtained product was calcined at 500 °C in air for 3 hr and the size range of the synthesized ZnO powder was approximately 20–40 nm.

Song *et al* [100] synthesized highly pure active γ-Al_2O_3 nanoparticles from aluminum nitrate and ammonium carbonate with a little surfactant by chemical precipitation method. The factors that affected the synthesis process were studied. The properties of γ-Al_2O_3 nanoparticles were characterized by DTA, XRD, BET, TEM, laser granularity analysis and impurity content analysis. The authors reported that amorphous precursor of $Al(OH)_3$ sols are produced by using 0.1 mol/L $Al(NO_3)_3 \cdot 9H_2O$ and 0.16 mol/L $(NH_4)_2CO_3 \cdot H_2O$ solutions, in the volume ratio 1:3, followed by addition of 0.024% (volume fraction) surfactant PEG600, and reacting at 40 °C, 1 000 r/min stirring rate for 15 min. Thereafter, stabilization was done for 24 h and the precursors were extracted and filtered by vacuum, washed thoroughly with deionized water and finally with dehydrated ethanol, and dried in vacuum at 80°C for 8 h. Finally, they were calcined at 800 °C for 1 h in the air, and high purity active γ-Al_2O_3 nanoparticles were obtained with about 9 nm in crystal grain size.

3. Sol–gel Synthesis

Sol–gel processing is also a promising method for the preparation of nano dimensional materials. It is most commonly used technique for the preparation of bulk nanomaterial of Metal Oxides [102]. The reaction product of the sol–gel synthesis could be either colloidal powders or films. One of the advantages of this method is the ability to control the microstructure of final product by controlling chemical reaction parameters [103]. It involves the evolution of networks through the formation of colloidal suspension (sol) and gelatin to form a network in continuous liquid phase (gel). The precursor for synthesizing these colloids could be either inorganic salts or organic compounds known as metal alkoxides and aloxysilanes. The most widely used are tetramethoxysilane (TMOS), and tetraethoxysilanes (TEOS) which form silica gels. The sol gel process involves initially a homogeneous solution of one or more selected alkoxides. These are organic precursors for silica, alumina, titania, zirconia, among others [104]. A catalyst is used to start reaction and control pH. Sol-gel formation occurs in four stages.

- Hydrolysis
- Condensation
- Growth of particles
- Agglomeration of particles

Hydrolysis

In hydrolysis, alkoxide groups (OR) are replaced by (OH) of water molecules and metal hydroxide is formed according to the equation below [105, 106].

$$M\text{-}O\text{-}R + H_2O \rightarrow M\text{-}OH + ROH$$
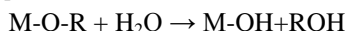
For example, in the formation of silica gel, hydrolysis occurs by attack of oxygen on silicon atoms. This can be accelerated by addition of a catalyst such as HCl and NH_3. Hydrolysis continues until all alkoxy groups are replaced by hydroxyl groups. Subsequent condensation involving silanol group (Si-OH) produced siloxane bonds (Si- O-Si), alcohol and water [105]. Hydrolysis occurs by attack of oxygen contained in the water on the silicon atom. Using tertraethoxysilane, the hydrolytic step can be described with the following reaction;
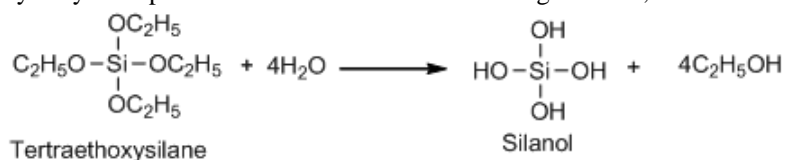
Condensation

In condensation two hydroxylated species react to form M-O-M bonds under release of water molecules (oxolation). Finally reaction between hydroxide and Alkoxide produces M-O-M bonds with release of alcohol molecule. Condensation as shown below [105, 106];

M-OH+ H-O-M $\rightarrow$ M-O-M + H_2O (oxolation)

M-OR + M-OH $\rightarrow$ M-O-M + R-OH
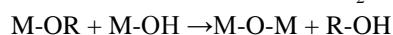
For sol gel formation, polymerization to form siloxane bond occurs by either a water producing or alcohol producing condensation reaction. The end result of condensation products is the formation of monomer, dimer, cyclic tetramer, and high order rings. The rate of hydrolysis is affected by pH, reagent concentration and H_2O/Si molar ratio (in case of silica gels). Also ageing and drying are important. By control of these factors, it is possible to vary the structure and properties of sol-gel derived inorganic networks.

The reaction for the condensation step is shown below;

OR
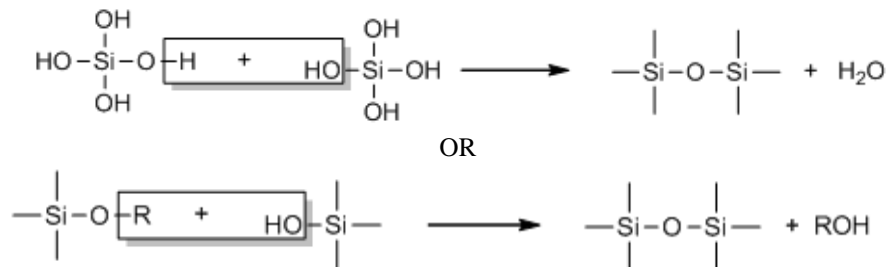
Growth and Agglomeration

As the number of siloxane bonds increase, the molecules aggregate in the solution, where they form a network, a gel is formed upon drying. The water and alcohol are driven off and the network shrinks.

The physical characteristic of the gel network depends greatly on the size of the particles and the extend of cross-linking prior to the gelation.

S. Ramesh [104] described the synthesis of $Ag_{3\ (2+x)}Al_xTi_{4-x}O_{11+\delta}$ ($0.0 \leq x \leq 1.0$) nanoparticles. These nanoparticles were prepared by the sol-gel technology and the procedure used by the author is given thus; The calculated amounts of $Al(NO_3)_3$, $Ag(NO_3)_2$ and TiO_2 were mixed in $2\,mol.L^{-1}$ nitric acid with continuous stirring for 1 h at pH of about 4-5, followed by addition of 30mL of $1.5\,mol\ L^{-1}$ citric acid solution. The resulting solution changed to a yellowish sol and the stirring continued with the aid of a magnetic stirrer at $60^{\circ}C$ until it became a transparent sticky gel. Thereafter, the gel was dried in an air oven at $200^{\circ}C$ for 1 h and this led to the formation of a light weight porous materials due to the enormous gas evolution and it was sintered at $850^{\circ}C$ for 4h to get the fine homogeneous dense powder. A pictorial representation of the synthesis method is given in Figure 1.
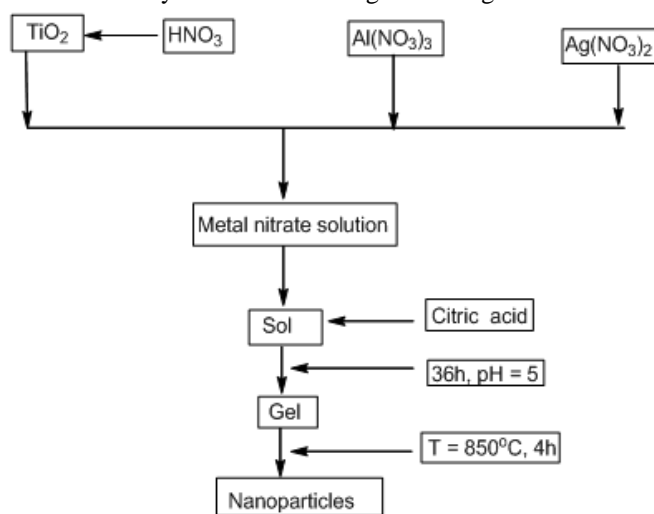
Figure 14: Flow chart of sample preparation of $Ag_{3\ (2+x)}Al_xTi_{4-x}O_{11+\delta}$ ($0.0 \leq x \leq 1.0$) nanoparticles

Hasnidawani *et al* [105] synthesized ZnO nanoparticles via sol gel method using Zinc acetate dehydrate ($Zn(CH_3COO)_2.2H_2O$) as a precursor and ethanol (C_2H_5OH) as solvent, while sodium hydroxide (NaOH) and distilled water were used as the reaction medium. ZnO nanoparticles were characterized by using XRD, EDX, FESEM, and nano-particles analyser. The nanosizes of the ZnO nanoparticles synthesized ranged within 81.28nm to 84.98nm. Below is the FE-SEM micrograph of zinc oxide synthesized in different magnification.

Figure 15: FE-SEM micrograph of zinc oxide synthesized in different magnification

The complete hydrolysis of zinc acetate with NaOH in an ethanolic solution resulted in the formation of a ZnO colloid [105]. The final product was obtained as a result of the equilibrium between the hydrolysis and condensation reaction. Due to the heating, Zinc Acetate within the solution underwent hydrolysis forming acetate ions and zinc ions. The abundance of electrons in the oxygen atoms made the hydroxyl groups (-OH) of alcohol molecules bond with the zinc ions. The overall chemical reaction for the formation of ZnO nano-powder when sodium hydroxide was used as solvent is shown below;

$$(Zn (CH_3COO)_2. 2H_2O) + 2NaOH \rightarrow \quad ZnO + 2NaCH_3COO + H_2O$$

According to Umbreen and Bushra [106] Nanoparticles of nickel Oxide has been synthesized by Sol-Gel method. In the first step Nanosols were prepared by dissolving metal salt in suitable Solvent. On condensation Nanosols were converted into Nanostructured Gel of Nickle oxide nanoparticles was found to be 8.78 nm

The procedure adopted by these authors is given thus; $NiCl_2.6H_2O$ (1.5g) was transferred into a 250 ml round bottom flask at room temperature and absolute alcohol (70 ml) was added to the flask. The content of the flask was subjected to continuous stirring. Thereafter, NaOH (0.5 g) was dissolved in absolute alcohol (100 ml) in another beaker and this solution was added to $NiCl_2.6H_2O$ solution drop wise. The mixture was stirred for 2hours and a light greenish colored gel was formed. The gel was allowed to stand for three hours and then filtered and washed with water and finally with ethanol to give a light green colored precipitate. The precipitate was then oven dried at 100 ºC for 2 hours to yield fine green powder which was subjected to calcination at 290 ºC for 30 minutes. Black colored NiO nanopowder of was formed after calcination.

3.1. Sonochemical Synthesis

Currently, ultrasound irradiation has become an important tool in chemistry. It provides an unusual mechanism for generating high-energy chemistry with extremely high local temperatures and pressures and an extraordinary heating and cooling rate [107].

Sonochemistry drives principally from acoustic cavitations which involve the formation, growth and implosive collapse of bubbles in liquids. When solutions are exposed to strong ultrasound irradiation, bubbles are implosively collapsed by acoustic fields in the solution. High temperature and high-pressure fields are produced at the centers of the bubbles. The implosive collapse of the bubbles generates a localized hotspot through adiabatic compression or shock wave formation within the gas phase of the collapsing bubbles [107]. The conditions formed in these hotspots have been experimentally determined, with the transient temperature of ~5000 K, pressure of > 1800 atm and cooling rates in excess of 1010 M/s. These extreme conditions enable many chemical reactions to occur. The products are sometimes nano amorphous particles and, in other cases, nanocrystalline [108, 109].

Narendra and Sunita [110] reported the synthesis of the following inorganic Nanopaticles by Sonolysis;

(i) Nanomatallic Powder: This could be obtained by the sonocation of metal carbonyls. For example Fe powder could be obtained from $Fe(CO)_5$, Ni from $Ni(CO)_4$, Co from $Co(CO)_3NO$, Pd from $Pd(O_2CCH_3)_2)$. The above authors also claimed that the sonocation of divalent salt of Pd(II) (1.0Mm) solution in polyethylene glycol monostearate solution could furnish about 5-nm Pd particles with fairly narrow distribution while using K_2PdCl_4 or

H_2PtCl_6 solution could result in the formation of nano-Pd and nano-Pt particles of size 3.6±0.7nm Pd under Ar and 2.0±0.3nm Pt under N_2 stream respectively [110].

(ii) Nanometal Alloy: The synthesis of metal alloy NPs using a combination of metal and salts/complexes as precursor material via sonolysis was also reported by the above authors. These include

(a) Amorphous Fe/Co which could be obtained from a mixture of $Fe(CO)_5$ and $Co(CO)_3NO$ in decalin;

(b) M50 steel powder with extremely high hardness which could be obtained from $Fe(CO)_5$, $(EtxC_6H_6-x)_2Mo$, and $V(CO)_6$ in decalin;

(c) Au/Pd which could be obtained from $NaAuCl_4$ and $PdCl_2$, this appears as a monodisperse distribution (8nm) with gold core and Pd shell.

(e) Ag/Fe_2O_3 could be obtained from $AgNO_3$ and $Fe(CO)_5$, Fe/Ni/Co from $Fe(CO)_5$, $Ni(CO)_4$, and $Co(CO)_3NO$ [110].

A typical preparation procedure for $Fe_{40}Co_{60}$ alloy is given below as was reported by the above authors;

Under an argon atmosphere by means of an ultrasonic device with direct immersion titanium horn (working frequency 20 kHz, electrical power of generator 600W, irradiation surface area of the horn 1cm^2), 2.0 ml $Fe(CO)_5$ (0.15M) and 1.5 ml $Co(CO)_3NO$ (0.15M) were dissolved in 100 ml diphenlmethane for 3h at 20-30°C. A black solid product was obtained, separated by centrifugation, washed with pentane inside the N_2- filled glove box and dried under vacuum at room temperature. This was followed by the annealing of the solid under an argon flow (99.996%) for 5h at 600°C to give about 60% $Fe_{40}Co_{60}$ alloy by weight [110].

3.2. Solvothermal Decomposition of Metal Complexes

One of the simplest methods to prepare nanoparticles is the decomposition of organometallic precursors. This decomposition may be driven by heat (thermolysis), light (photolysis), and sound (sonolysis). In most cases organometallic compounds are used in this method of nanoparticles synthesis and the major advantage of using organometallic compounds is that the precursors can be decomposed at relatively low temperatures to form the final product. Also by controlling the decomposition temperature, the growth of the nanoparticles can be controlled [110]. Since size and morphology have an effect on the properties of the nanoparticles, control of these properties is a primary goal. In many cases, polymers, organic capping agents, or structural hosts are used to limit the size of the nanoparticle growth [111]. In line with the above, Chen and Lee [112] used surfactant sodium dodecyl benzenesulfonate (SDBS) as surfactant which also acted as stabilizer during hydrothermal reduction of $CuCl_2 .2H_2O$ to produce various shapes and structures of copper nanoparticles which greatly depended upon the reaction temperatures and quantity of SDBS [113].

Divine *et al* [114] prepared CdO nanoparticles by the thermal decomposition of a precursor complex through a simple and cost effective room temperature synthetic technique. This method allows the preparation of the precursor complex from hexamethylenetetramine and cadmium nitrate in ethanol. The procedure employed by the authors is given thus; a sample of the dry precursor (0.5 g) was ground, placed in a ceramic crucible and calcined at 500 °C (CdO-500). The crucible was placed in the furnace, heated to the desired calcination temperature, and calcination in air for 2 h. Thereafter the sample was allowed to cool to room temperature in the furnace and reddish-brown powder cadmium oxide nanoparticles were obtained.

Jonglak and Edward [115] solvothermally moderated the synthesis and decomposition of metal azide to produce nanocrystalline mid to late transition metal nitrides. Several of these nitrides were discovered to be thermally metastable and decompose at temperatures below ~500 °C. This method utilizes exothermic metathesis reactions between metal halides ($NiBr_2$, $FeCl_3$, $MnCl_2$) and sodium azide in superheated toluene at temperatures below 300 °C to synthesize nanocrystalline hexagonal Ni_3N and Fe_2N, and tetragonal MnN.

3.3. Microwave Synthesis

The interaction of dielectric materials, liquids or solids, with microwaves has given rise to what is generally known as dielectric heating. Electric dipoles present in such materials respond to the applied electric field. In liquids, constant reorientation leads to the friction between molecules, which subsequently generate heat energy [116,]. The

microwave irradiation has been used in the synthesis of inorganic nanoparticles and keeps showing rapid growth in its application in material science. Microwaves are a form of electromagnetic energy, with frequencies in the range of 300MHz to 300 GHz but the commonly used frequency is 2.456 GHz [117].

Blosi *et al* [116] reported microwave-assisted polyol synthesis of crystalline particles with radius ranging from 90nm to 260nm. Very smaller sized- nanoparticles can be synthesized in cases where microwave is applied to the reaction solution. The same author also reported synthesis of copper nanoparticles using microwave-assisted synthesis [75]. The main reasons for using microwave are the fast and homogeneous reaction conditions during the microwave synthesis.

Zhu and Yin [117] reported a fast method for the production of copper nanoparticles by using copper sulphate as a precursor and sodium hypophosphite as the reducing agent in ethyl glycol under microwave irradiation. They are also studied the parameters like concentration of reducing agent and microwave irradiation time. The size of copper nanoparticles prepared by this method was about 10 nm [76].

Ashok and Umesh [118] reported the synthesis of SnO_2 nanoparticles (NPs) using microwave method. The procedure adopted by the above author is described thus; 0.03 M solution of $SnCl_2$.$2HO_2$ was prepared and 0.05 M citric acid mixed in to it drop wise. This solution was heated at $80^{o}C$ in oven till becomes 1/4th of its volume . Thereafter, the precursor was kept for microwave heating for 10 min at 700 watt to form precipitate . The precipitate obtained was filtered and washed 2-3 times with de -ionised water (18.2 MΩ. cm resistivity) then dried at $100^{o}C$ in an oven. The dried powder was crushed and annealed at $500^{o}C$ for 1 hr. to give SnO_2 nanoparticles.

Kozakova *et al* [119] prepared spherical Fe_3O_4 nanoparticles using microwave method. The particles obtained were uniform with average dimensions of 200 nm and exhibit ferromagnetic behavior dependent on synthesis temperature. The procedure adopted by the authors is given thus; 5mmol of $FeCl_3.6H_2O$ was dissolved in 60mL of ethylene glycol, followed by the addition of nucleating agent (50mmol of NH_4Ac, 25mmol of $(NH_4)_2CO_3$ or 200mmol of aqueous NH_3). This mixture was placed in a Teflon reaction vessel (XP-1500 Plus heated in pressurized CEM Mars 5 microwave system (CEM Corporation) to a required temperature (200, 210 or $220^{o}C$) maintains for 30 min. After the reaction, the vessel was cooled to room temperature and the obtained product was filtered off, washed with water and ethanol for several times and dried naturally on air.

3.4. Biological Synthesis

Nature has various synthetic processes for nanoparticles and micro-length scaled inorganic materials. This has led to the development of a new area of research which is based on the biosynthesis of nanomaterials [120]. Biosynthesis of nanoparticles has gained popularity recently because of the costly and hazardous nature of the physical and chemical processes. It involves the use of microorganisms and plant extracts for synthesis. It is considered to be a bottom-up approach and it involves oxidation-reduction (redox) processes where metallic compounds are usually reduce into their respective nanoparticles because of microbial enzymes activity or the plant phytochemicals with antioxidant or reducing properties [121]. There are three important factors that should be considered in the application of this method and they include the choice of (a) the solvent medium used, (b) reducing agent and (c) a nontoxic material for the stabilization of the nanoparticles [109].

Bacteria, actinomycetes, fungi and plant extracts have been used and are in use for the synthesis of nanoparticles [120] The major advantages of this method is that it involves very easy procedures and less toxicity with a wide range of applications of nanoparticles produced according to their morphology.

Biomolecules, including DNA [121, 122] and polyproteins such as amyloid fibers [123], peptide nanotubes [124], and F-actin [125], have been used as templates to grow metallic "biowires" through the catalytic reduction of copper, gold, and silver ions. Metallization has been initiated either directly from electrostatically associated ions or by covalently bound metal nanoparticle seeds. Through metallization, Behrens and co-workers [126] assembled silver NP ring structures using tubulin as template, and Mukherjee *et al.* [127] assemble Au NPs in a rod- like fashion using tubulin as template.

In another development, silver nanoparticles (AgNP) were synthesized by Anamika *et al* [128] by using aqueous extract of *Moringa oleifera* and aqueous solution of silver nitrate ($AgNO_3$).

The table below shows some biological entities and the Nanoparticles synthesized as adopted from [110].

Table 1: biological entities and the Nanoparticles synthesized

Biological Entity	NPs Synthesized
Bacteria	**Size**
Bacillus magatherium	Au (15-30nm)
Bacillus subtilis	Ag (0.5-60nm)
Brevibacterium casei	Ag (50nm)
Enterobacteria cloacae	Ag (50-100nm)
Eschericha coli	Ag (05-25nm)
Kllebsiella pneumonia	Ag (50nm)
Actinomycete	
Thermomnospora sp	Au (0.8nm)
Fungi	
Aspergergillus clavatus	Ag (10-25nm)
Aspergergillus flavus	Ag (0.7-10nm)
Aspergergilus fumigates	Ag (0.5-25)
Colletotrichum sp	Au (20-40nm)
Fusarium oxysporum	Ag (20-25nm)
Fusarium oxysporum	Au (20-40nm)
Plant Leaves Extract	
Aloe vera sp	Ag, Au (15-20nm)
Azadirachta indica	Ag, Au, Ag-Au (50-100nm)
Cymbopogon flexuosus	Au (0.05-2nm)
Pelargoncium gravcolens	Au (20-40nm)
Tamarindus indica	Au (20-40)
Stem/bark/latex	
Cinnamomum zeylanicum	Ag (50-100nm)
Desmodium triflorum	Ag (0.5-20nm)
Jatropha curcas	Ag (10-20)
Pelargoncum gravcolens	Au (8-24nm)
Fruit extract	
Cariaca papaya	Ag (20-40)
Emblica officinalis	Au (15-20nm)
Root extract	
Curculigo orchioides	Ag (20-40nm)
Pelargoncum gravcolens	Au (11-34)

4. Conclusion

Nanostructured materials have been extensively studied during the last decade due to their wide range of applications. From the above review, it can be observed that the field of nanomaterials and their methods of production are very dynamic. Research areas in the field of nanosciences and nanotechnologies which gives rise to the production of Nanoparticles, Nanorods, nanofibers as well as mesoporous nanoporous structures have been developed. In this review, we have pointed out the different synthetic methods of producing nanostructured materials. Some of them are very efficient and lead to high yields, relatively short reaction times, and low cost,

simple experimental and isolation procedures while some are not. These nanomaterials show size-dependent as well as shape and structure-dependent, optical, electronic, thermal, and structural properties.

References

1. S. Iravani, H. Korbekandi, S.V. Mirmohammadi and B. Zolfaghari (2014) Synthesis of silver nanoparticles: chemical, physical and biological methods". *Research in Pharmaceutical Sciences*, 9(6), 385-406
2. Colvin VL, Schlamp MC, Alivisatos; (1999); A Light emitting diodes made from cadmium selenide nanocrystals and a semiconducting polymer". *Nature;* 370, 354-357
3. Wang Y, and Herron N. (1991), "Nanometer-sized Semiconductor Clusters: Materials Synthesis, Quantum Size Effects, and Photophysical Properties". *J. Phys Chem*.; 95, 525-532
4. Schmid G. (1992) "Large Clusters and Colloids.Metals in the Embryonic State". *Chem Rev;* 92, 1709-1027.
5. Hoffman AJ, Mills G, Yee H, Hoffmann M. (1992), "Q-sized Cadmium Sulfide: Synthesis, Characterization, and Efficiency of Photo-initiation of Polymerization of Several Vinylic Monomers. *J. Phys Chem*.; 96, 5546-5552.
6. Hamilton JF, Baetzold R (2005), "Catalysis by Small Metal Clusters", *Science;* 205,2005, :1213-1220
7. Mansur HS, Grieser F, Marychurch MS, Biggs S, Urquhart RS, Furlong D.(1995) Photo-electrochemical properties of '   Q-state' Cds particles in Arachidic acid Langmuir-blodgett Films. *J. Chem Soc. Faraday Trans.*; 91, :665-672.
8. Mamalis, A.G., Vogtländer, L.O.G., and Markopoulos, A. (2004) Nanotechnology and nanostructured materials: trends in carbon nanotubes. *Precision Engineering*, 28, pp. 16-30.
9. Klabunde, K.J. (2001) Nanoscale Materials in Chemistry. New York, Wiley-Interscience.
10. Bell, A.T. (2003): The Impact of Nanoscience on Heterogeneous Catalysis. *Science*, 299(5613), pp. 1688-1691
11. Grunes, J., Zhu, J., and Somorjai, G.A. (2003) Catalysis and Nanoscience. *Chem. Comm*., pp. 2257-2260.
12. Jiang, L. Q.; Gao, L. (2005), Fabrication and characterization of ZnO-coated multiwalled carbon nanotubes with enhanced photocatalytic activity. *Mater. Chem. Phys.*, *91,* 313-316.
13. Narenda Kumar and Sunita Kumbhat (2016), "Essentials in Nanoscience and Nanotechnology" Published 2016 by John Wily & Sons, Inc, pp 31-74
14. Thakur Prasad Yadav, Ram Manohar Yadav, Dinesh Pratap Singh (2012), Mechanical Milling: a Top Down Approach for the Synthesis of Nanomaterials and Nanocomposites, *Nanoscience and Nanotechnology*, 2(3): 22-48 DOI: 10.5923/j.nn.20120203.01
15. Natalia L. Pacioni, Claudio D. Borsarelli, Valentina Rey and Alicia V. Veglia (2015), Synthetic Routes for the Preparation of Silver Nanoparticles. A Mechanistic Perspective © Springer International Publishing Switzerland 2015 E.I. Alarcon *et al*. (eds.), Silver Nanoparticle Applications, Engineering Materials, DOI 10.1007/978-3-319-11262-6-2.
16. O. Masala and R. Seshadri (2004), "Synthesis Routes for Large Volumes of Nanopacticles", *Ann. Rev. Mater.Res.*34, 41-81
17. L.S. Wang and R.Y. Hong (2011) "Synthesis, Surface Modification and Characterization of Nanoparticles", Advances in Nanocomposites-Synthesis, Characterization and Industrial Applications, Ed. B. Reddy, InTech, www.intechopen.com.
18. E. Gaffet, M. Tachikart, O. El Kedim, R. Rahouadj (1996), "Nanostructural materials formation by mechanical alloying: morphologic analysis based on transmission and scanning electron microscopic observations", *Mater. Charact*., 36, 185–190.
19. J. D. Aiken III, R. G. Finke (1999). A Review of Modern Transition-Metal Nanoclusters: Their Synthesis, Characterization, and Applications in Catalysis, *J. Mol. Catal.* 145, 1–44.
20. Hamid Reza Ghorbani (2014) "A Review of Methods for Synthesis of Al Nanoparticles" *Orient. J. Chem.,* Vol. 30(4), 1941-1949 (2014)

21. Shoshin, Y. L.; Mudryy, R. S.; Dreizin, E. L. (2002), *Combust. Flame*, *128*, 259-269.
22. Dreizin, E. L.; Shoshin, Y. L.; Mudryy, R. S. (2001), CPIA *Publication*, *705*, 189-199.
23. Pivkina A., Streletskii A., Kolbanev I., Ul'yanova P., Frolov Y., Butyagin P., Schoonman J (2004)., *J. Mater. Sci.*, *39*, 5451-5453.
24. J. Sun, J.X. Zhang, Y.Y. Fu, and G.X. Hu, Materials Science and Engineering A 329-331, 703 (2002).
25. I. Manna, P.P. Chattopadhyay, F. Banhart, and H.J. Fecht, Materials Science and Engineering A 379, 360 (2004)
26. T. Spassov, P. Solsona, S. Bliznakov, S. Suriñach, and M.D. Baro, Journal of Alloys and Compounds 356–357, 639 (2003)
27. J.S. Lee, C.S. Lee, S.T. Oh, and J.G. Kim, Scripta mater. 44, 2023 (2001)
28. H. S. Park , D. H. Kim, S. J. Kim, and K. S. Lee, Journal of Alloys and Compounds, 415, 51 (2006)
29. M. Paskevicius, J. Webbb, M.P. Pitt, T.P. Blach, B.C. Hauback, E.MacA. Gray, C.E. Buckley, (2009) *Journal of Alloys and Compounds*, 481, 595–599.
30. Munnings, C.; Badwal, S. P. S.; Fini, D. (20 February 2014). "Spontaneous stress-induced oxidation of Ce ions in Gd-doped ceria at room temperature"*, Ionics. 20 (8):* 1117–1126. doi*:10.1007/s11581-014-1079-2.*
31. Eugene G. Avvakumov and Lembit G. karakchiev (2004), Mechanochemical Synthesis as a Method for the Preparation of Nanodisperse Particles of Oxide Materials: *Chemistry for Sustainable Development* 12 (2004) 287-291
32. Takuya Tsuzuki, Paul G. McCormick (2004), Mechanochemical synthesis of nanoparticles. *Journal of Materials Science* 39, 5143 – 5146.
33. T. Tsuzuki and P. G. McCormick, *Nanostr. Mater.* 12 (1999) 75.
34. T. Tsuzuki, J. Ding and P. G. McCormick, *Physica B*, 239 (1997) 378.
35. T. Tsuzuki and P. G. McCormick, *Appl. Phys.* A, 65 (1997) 607
36. T. A. Schoolcraft and B. J. Garrison, Journal of the American Chemical Society (1991). "Initial Stages of Etching of the Silicon Si110 2x1 Surfaces by 3.0-eV Normal Incident Fluorine Atoms: A Molecular Dynamics Study". *Journal of the American Chemical Society,* 113 (22): 8221.
37. Marwa Nabil and Hussien A. Motawah (2015), Silica Nanoparticle preparation using alkaline etching process; Applied Mechanics and Materials, 749, 155-158.
38. Wei Cheng, Weidong Zhang, Lijuan Hu, Wei Ding, Feng Wu and Jinjun Li (2016), Etching synthesis of iron oxide nanoparticles for adsorption of arsenic from water; *RSC Adv.*, 6, 15900-15910 DOI: 10.1039/C5RA26143K
39. Kwangjin An, Soon Gu Kwon, Mihyun Park, Hyon Bin Na, Sung-Il Baik, Jung Ho Yu, Dokyoon Kim, Jae Sung Son, Young Woon Kim, In Chan Song, Woo Kyung Moon, Hyun Min Park and Taeghwan Hyeo (2008), Synthesis of Uniform Hollow Oxide Nanoparticles through Nanoscale Acid Etching *Nano Lett.*, 8 (12), pp 4252–4258. DOI: 10.1021/nl8019467
40. Min Nie, Kai Sun, and Dennis Desheng Meng (2009), Formation of metal nanoparticles by short-distance sputter deposition in a reactive ion etching chamber. *Journal of Applied Physics* 106, 05431
41. J. Küppers (1995). "The hydrogen surface chemistry of carbon as a plasma facing material" *Surface Science Reports,* 22 (7–8): 249
42. http://www.spts.com/uploaded_files/1093/images/HF-Intro-A4.pdf, 21/11/2016.
43. R. Behrisch (ed.) (1981). Sputtering by Particle bombardment; *Springer Berlin* ISBN 978-3-540-10521-3
44. M. Sporn; Libiseller, G.; Neidhart, T.; Schmid, M.; Aumayr, F.; Winter, HP.; Varga, P.; Grether, M.; Niemann, D.; Stolterfoht, N.; *et al.* (1997). "Potential Sputtering of Clean SiO_2 by Slow Highly Charged Ions". *Physical Review Letters,* 79 (5): 945.
45. M.W. Thompson (1962). "Energy spectrum of ejected atoms during the high- energy sputtering of gold" *Philos. Mag.* 18 (152): 377.
46. R. Behrisch and W. Eckstein (eds.) (2007). Sputtering by Particle bombardment; Experiments and Computer Calculations from Threshold to Mev Energies; *Springer,,Berlin.*

47. R. Perekrestov, P. Kudrna, M. Tichý (2013), Deposition of TiO_2 Nanoparticles by Means of Hollow Cathode Plasma Jet .WDS'13 Proceedings of Contributed Papers, Part II, 139–143, 2013.

48. W. Cao; Synthesis of Nanomaterials by Laser Ablation. Skyspring Nanomaterials, Inc. http://www.ssnano.com, wcao@ssnano.com 22/11/16

49. Patra A, Métivier R, Piard J, Nakatani K.(2010), SHG-Active Molecular Nanorods with Intermediate Photochromic Properties Compared to Solution and Bulk Solid States. *Chemical Communications*; 46 (34) 6385-6387

50. Liu M. Ji Z., Shang L (2010). Part One Top-Down Strategy: Top-Down Fabrication of Nanostructures. In: Chi L. (ed.) Nanotechnology: Volume 8: Nanostructured Surfaces: Weinheim,

51. Bondi SN, Lackey WJ, Johnson RW, Wang X, Wang ZL (2006). Laser Assisted Chemical Vapor Deposition, Synthesis of carbon Nanotubes and their Characterization. *Carbon*; 44 1393-403.

52. Chen C, Chen W, Zhang Y. (2005), Synthesis of Carbon Nano-tubes by Pulsed Laser Ablation at Normal Pressure in Metal Nano-sol. Physica E: Low-dimensional Systems and Nanostructures; 28 (2) 121-27.

53. Fukata N, Oshima T, Tsurui T, Ito S, Murakami K. (2005), Synthesis of silicon nanowires using laser ablation method and their manipulation by electron beam. *Science and Technology of Advanced Materials*; 6 (6) 628-32.

54. Prashant K, Panchakarla LS, Rao (2011), CNR. Laser-Induced Unzipping of Carbon Nanotubes to Yield Graphene Nanoribbons. *Nanoscale*; 3(5) 2127-2129

55. Russo P, Hu A, Compagnini G, Duley WW, Zhou NY, (2014). Femtosecond Laser Ablation of Highly Oriented Pyrolytic Graphite: A green route for large-scale production of porous graphene and graphene quantum dots. *Nanoscale*; 6 (4) 2381-2389.

56. Anikin KV, Melnik NN, Simakin AV, Shafeev GA, Voronov VV, Vitukhnovsky AG (2014). Formation of ZnSe and CdS quantum dots via laser ablation in liquids; *Chemical Physics Letters*. 366 (3-4) 357-360.

57. Semaltianos N, Logothetidis S, Perrie W, Romani S, Potter R, Sharp M, French P, Dearden G, Watkins K (2008). CdSe Nanoparticles Synthesized by Laser Ablation. *EPL (Europhysics Letters);* 84 (4) 47001

58. Wesolowski MJ, Kuzmin S, Wales B, Sanderson JH, Duley WW, (2013). Self-assembly of thin Carbon Micro-Shells through Pulsed Laser Irradiation of a Ferrocene/benzene solution; *Journal of Materials Science*; 48 (18) 6212-6217

59. Patil P, Phase D, Kulkarni S, Ghaisas S, Kulkarni S, Kanetkar S, Ogale SBhideV. (1987), Pulsed-Laser–Induced Reactive Quenching at Lliquid-Solid Interface: Aqueous oxidation of iron. *Physical Review Letters*; 58 (3) 238-241.

60. Geraint Williams and Gary S. V. Coles (1998), Gas sensing properties of nanocrystalline metal oxide powders produced by a laser evaporation technique , *J. Mater. Chem.*, 1998,8, 1657-1664 DOI: 10.1039/A802006J

61. Geraint Williams and Gary S. V. Coles (1999), Gas Sensing Potential of Nanocrystalline Tin Oxide Produced by a Laser Ablation Technique. Article in *MRS Bulletin* 24(6):25-29 · June 1999 DOI: 10.1557/S0883769400052477

62. Starke T.K.H and Cole G.S.V. (2002)" High Sensitive Ozone Sensor for Environmental Monitoring using Laser ablated nanocrystalline Metal Oxides, *IEEE Sen. J.* 2, 14-19

63. Lue, Juh Tzeng, (2007), "Physical properties of nanomaterials", *Encyclopedia of nanosci. & nanotech.*, Vol. 10, pp 1-46.

64. Hasany, S.F., Ahmad, I., Ranjan, J. & Rehman, A., (2012) "Systematic review of the preparation techniques of Iron oxide Magnetic Nanoparticles", *Nanoscience & Nanotechnology*, Vol. 2(6), pp148-158.

65. Namita Rajput (2015)," Methods of Preparation of Nanoparticles – A Review. *International Journal of Advances in Engineering & Technology*, Vol. 7, Issue 4, pp. 1806-1811

66. Tissue, B.M. and Yuan H.B. (2003) " Structure particle size and annealing gas phase-condensed Eu^{3+} : Y_2O_3 nanophosphors ", *J. Solid State Chemistry*, Vol. 171, pp12- 18.

67.   Wesley O. Gordon, John R. Morris, Brian M. Tissue (2009), Control of morphology in inert-gas condensation of metal oxide nanoparticles , *Journal of Materials Science*, Volume 44, <u>Issue 16</u>, pp 4286–4295

68.   M B Ward, R Brydson and R F Cochrane (2006) Mn nanoparticles produced by inert gas condensation, *Journal of Physics*: Conference Series 26, 296–299

69.   Namita Rajput (2015)," Methods of Preparation of Nanoparticles – A Review. *International Journal of Advances in Engineering & Technology*, Vol. 7, Issue 4, pp. 1806-1811

70.   R. Schmechel, M. Kennedy, H. von Seggern, H. Winkler, M. Kolbe, R. A. Fischer, Li Xaomao, A. Benker, M. Winterer and H. Hahn (2001), Luminescence properties of nanocrystalline Y2O3:Eu^{3+} in different host materials. *J. Appl. Phys*. 89, 1679 http://dx.doi.org/10.1063/1.1333033

71.   Robert A. Senter , Yandong Chen , and Jeffery L. Coffer (2001). Synthesis of Silicon Nanocrystals with Erbium-Rich Surface Layers. *Nano Letters*, 1 (7), pp 383–386

72.   Joachim U. Brehm , Markus Winterer and Horst Hahn (2006); Synthesis and local structure of doped nanocrystalline zinc oxides. *J. Appl. Phys*. 100, 064311

73.   Wang, J.W. and Y.D. Li, Synthesis of single-crystalline nanobelts of ternary bismuth oxide bromide with different compositions. Chemical Communications, 2003(18): p. 2320-2321.

74.   Liu, H., C.G. Hu, and Z.L. Wang, Composite-hydroxide-mediated approach for the synthesis of nanostructures of complex functional-oxides. Nano Letters, 2006. 6(7): p. 1535-1540.

75.   Wang, X.D., *et al*., Large-scale synthesis of six-nanometer-wide ZnO nanobelts. Journal of Physical Chemistry B, 2004. 108(26): p. 8773-8777.

76.   Zu Rong Dai, Zheng Wei Pan and Zhong L. Wang (2003), Novel Nanostructures of Functional Oxides Synthesized by Thermal Evaporation. *Advanced Functional Material*, 13, (1): p 9-24.

77.   Gohil, S., Chandra, R., Chalke, B., Bose, S. & Ayyub, P.,(2007) "Sputter Deposition of Self-Organised Nanoclusters through Porous Anodic Alumina Templates", *J. Nanoscience Nanotech*., 7(7) pp 641-646.

78.   Chang, W., Skandan, G., Hahn, H., Danforth, S.C. and Kear, B.H., (1994)" Chemical Vapor Condensation of nanostructured ceramic powders", *Nanostructured Materials,* vol. 4(3), pp 345- 351.

79.   Winterer, M. and Hahn, H., Metallkd, Z., (2003)" Chemical Vapor Synthesis of Nanocrystalline Powders ", *Nanoceramics by Chemical Vapor Synthesis*; vol 94, pp 1084-1090

80.   Anthony C. Jones and Michael L. Hitchman (2009), Overview of Chemical Vapor Deposition; Chemical Vapor Deposition: Precursors, Processes and Applications Edited by Anthony C. Jones and Michael L. Hitchman © Royal Society of Chemistry 2009 Published by the Royal Society of Chemistry, www.rsc.org

81.   Jing Kong, Alan M. Cassell, Hongjie Daia, (1998). Chemical vapor deposition of methane for single-walled carbon nanotubes. *Chemical Physics Letters*, 292, 567–574

82.   Pavel Moravec, Jiří Smolík, Helmi Keskinen, Jyrki M. Mäkelä, Snejana Bakardjieva, Valeri V. Levdansky (2011), NiO$_x$ Nanoparticle Synthesis by Chemical Vapor Deposition from Nickel Acetylacetonate; *Materials Sciences and Applications*, 2, 258-264 doi:10.4236/msa.2011.24033.

83.   G. Che, B. B. Lakshmi, C. R. Martin, and E. R. Fisher (1998), Chemical Vapor Deposition Based Synthesis of Carbon Nanotubes and Nanofibers Using a Template Method. *Chem. Mater*., 10,260-267

84.   Dr.   C.T.   John   Low;   Electrochemical   deposition   of nanomaterials https://ctjohnlow.wordpress.com/approaches/approaches-1/ 05/12/2016.

85.   Mohanty, U.S (2011), Electrodeposition: a versatile and inexpensive tool for the synthesis of nanoparticles, nanorods, nanowires, and nanoclusters of metals. *Journal of Applied Electrochemistry*, 41, (3), pp 257–270

86.   Injeti Gurrappa and Leo Binder (2008),   Electrodeposition of nanostructured coatings and their characterization—a review; *Sci. Technol. Adv. Mater*.9, 043001 (11pp)

87.   Park, H., Ayala, P., Deshusses, M.A. Mulchandani, A.,Choi, H., and Myung, N.V. (2008) Electrodeposition of maghemite (γ-Fe$_2$O$_3$) nanoparticles. Chemical Engineering Journal, 139, pp. 208-212.

88.   J.V. Zoval *et al*. (1996), "Electrochemical Deposition of Silver Nanocrystallites on the Atomically Smooth Graphite Basal Plane" *Journal of Physical Chemistry,* 100 pp. 837–844.

89.   R.T. Pötzschke *et al.,* "Nanoscale Studies of Electrodeposition on HOPG (0001)," *Electrochimica Acta,* 40 (1995), pp.1469–1474.

90.   G. Fasol and K. Runge, "Selective Electrodeposition of Nanometer Scale Magnetic Wires," *Applied Physics Letters,* 70 (1997), pp. 2467–2468.

91.   P. Aranda and J.M. García, "Porous Membranes for the Preparation of Magnetic Nanostructures," 249 (2002), pp. 214–219.

92.   T.M. Whitney *et al.,* "Fabrication and Magnetic Properties of Arrays of Metallic Nanowires," *Science,* 261 (1993), pp. 1316–1319.

93.   Laurier L. Schramm, Elaine N. Stasiuk and D. Gerrard Marangon (2003), Surfactants and their applications; *Annu. Rep. Prog. Chem., Sect. C*, 99, 3–48

94.   K. Shinoda, T. Nakagawa, B-I. Tamamushi and T. Isemura, Colloidal Surfactants, Some Physicochemical Properties, Academic Press, New York, 1963.

95.   Organized Solutions, Surfactants in Science and Technology, ed. S. E. Friberg and B. Lindman, Dekker, New York, 1992.

96.   Surfactants in Chemical/Process Engineering , ed. D. T. Wasan, M. E. Ginn and D. O. Shah, Dekker, New York, 1988

97.   Namita Rajput (2015)," Methods of Preparation of Nanoparticles – A Review. *International Journal of Advances in Engineering & Technology*, Vol. 7, Issue 4, pp. 1806-1811

98.   Y. Bahari Molla Mahaleh, S. K. Sadrnezhaad, and D. Hosseini (2008), NiO Nanoparticles Synthesis by Chemical Precipitation and Effect of Applied Surfactant on Distribution of Particle Size, *Journal of Nanomaterials* Volume 2008, Article ID 470595, pp 1-4 doi:10.1155/2008/470595.

99.   Hamid Reza Ghorbani, Ferdos Parsa Mehr, Hossein Pazoki and Behrad Mosavar Rahmani (2015) Synthesis of ZnO Nanoparticles by Precipitation Method; *Oriental Journal of Chemistry*, 31, (2): Pg. 1219-1221.

100.   T. Theivasanthi, N. Kartheeswari and M. Alagar, (2013) ; Chemical Precipitation Synthesis of Ferric Chloride Doped Zinc Sulphide Nanoparticles and Their Characterization Studies; *Chem. Sci Trans.* , 2(2), 497-507 .

101.   Song Xiao-lan, Qu Peng, Yang Hai-pin,   He Xi, Qiu Guan-zhou Synthesis of γ-Al$_2$O$_3$ nanoparticles by chemical precipitation method; Journal of Central South University of Technology October 2005, Volume 12, Issue 5, pp 536–541.

102.   Lu, C.H. and Jagannathan, J., (2002) "Cerium-ion-doped yttrium aluminum garnet nanophosphors prepared through sol-gel pyrolysis for luminescent lighting," *Applied Physics Letters*, vol.80 (19), pp 3608-3610.

103.   Morita, M., Rau, D., Kajiyama, S., Sakurai, T., Baba, M. and Iwamura, M., (2004) "Luminescence properties of nano-phosphors: metal-ion doped sol-gel silica glasses" *Materials Science-Poland*, vol.22 (1), pp 5-15.

104.   S. Ramesh (2013), Sol-Gel Synthesis and Characterization of Ag$_{3(2+x)}$ AlxTi$_{4-x}$O$_{11+\delta}$ $(0.0 \leq x \leq 1.0)$ Nanoparticles; Journal of Nanoscience Volume 2013, Article ID 929321, pp 1-9, http://dx.doi.org/10.1155/2013/929321

105.   J.N. Hasnidawani, H.N. Azlina, H. Norita1, N.N. Bonnia, S. Ratim and E.S. Ali (2016); Synthesis of ZnO Nanostructures Using Sol-Gel Method; *Procedia Chemistry;* 19, 211 – 216

106.   Umbreen Ashraf and Bushra Khan (2013): Synthesis and Characterization of NiO Nanopowder by Sol-Gel Method;   International Journal of Science and Research: 4(5), pp 2405-2408

107.   K. S. Suslick, T. Hyeon, M. Fang and Cichowlas (2012), Sonochemical Preparation of Nanostructured Selection of a Suitable Method for the Synthesis of Copper Nanoparticles NANO.07 Downloaded from www.worldscientific.com on 30/09/16, Catalyst, in Advanced Catalysts and Nanostructured Materials eds. W. R. Moser, Chap. 8 (Academic Press, New York, 1996).

108.   I. Haas and A. Gedanken, (2006). Sonoelectrochemistry of Cu in the presence of CTAB: Obtaining CuBr instead of Copper, *Chemistry of Materials* 15(5) 1184-1189.

109. Asim Umer, Shahid Naveed and Naveed Ramzan (2012)," Selection of a Suitable Method for the Synthesis of Copper Nanoparticles, NANO: *Brief Reports and Reviews* Vol. 7, No. 5

110. Narendra Kumar and Sunita Kumbhat (2016), Essentials in Nanoscience and Nanotechnology @ 2016 John Wiley & Sons Inc. Published by Jonh Wiley & Sons Inc. 30-70.

111. M. Byrappa and Yoshimura, (2001); Hydrothermal Technology- Principles and Applications, Handbook of Hydrothermal Technology (Noyes Publications, New Jersey, USA,

112. H. Chen and J. Lee, (2010) *J. Nanosci. Nanotechno*. 10,

113. K. Byrappa, (2005).Hydrothermal Processing, in Kirke-Othmer *Encyclopedia of Chemical Technology,* John Wiley and Sons, London.

114. Divine Mbom Yufanyi, Josepha Foba Tendo, Agwara Moise Ondoh & Joseph Ketcha Mbadcam (2014); CdO Nanoparticles by Thermal Decomposition of a Cadmium- Hexamethylenetetramine Complex; Journal of Materials Science Research; Vol. 3, No. 3; pp 1-11

115. Jonglak Choi and Edward G. Gillan (2009); Solvothermal Metal Azide Decomposition Routes to Nanocrystalline Metastable Nickel, Iron, and Manganese Nitrides; *Inorg. Chem.*, 48 (10), pp 4470–4477

116. M. Blosi, S. Albonetti, M. Dondi, C. Martelli and G. Baldi, J. Nanopart. (2011) *Res*. 13, 127 doi: 10.1007/s11051-010-0010-7.

117. H. T. Zhu, C.Y. Zhang and Y.-S. Yin, (2004), *J. Cryst. Growth* 270, 722.

118. Ashok K. Singh and Umesh T. Nakate (2013); Microwave Synthesis, Characterization and Photocatalytic Properties of SnO$_2$Nanoparticles; *Advances in Nanoparticles*, 2, 66-70.

119. Z. Kozakova, P. Bazant, M. Machovsky, V. Babayan and I. Kuritka (2010); Fast Microwave-Assisted Synthesis of Uniform Magnetic Nanoparticles; *Acta Physica Polonica A*, 118 (5), 948-949.

120. R. Bali, N. Razak, A. Lumb and A. T. Harris, (2006), The synthesis of Metal Nanoparticles Inside Live Plants, *IEEE Xplore*. 340592.

121. Changqing Yi, Dandan Liu and Mengsu Yang (2009)," Building Nanoscale Architectures by Directed Synthesis and Self-Assembly", *Current Nanoscience,* 2009*, 5,* 75-87 © 2009 Bentham Science Publishers Ltd.

122. Keren, K.; Krueger, M.; Gilad, R.; Ben-Yoseph, G.; Sivan, U.; Braun, E. (2002) Sequence-Specific Molecular Lithography on Single DNA Molecules. *Science*; 297, 72-75.

123. Scheibel, T.; Parthasarathy, R.; Sawicki, G.; Lin, X.; Jaeger, H.; Lindquist, S. L. (2003), Conducting Nanowires Built by Controlled Self-Assembly of Amyloid Fibers and Selective Metal Deposition. *Proc. Natl. Acad. Sci. USA, 100*, 4527-4532.

124. Reches, M.; Gazit, E (2003) Casting metal nanowires within discrete selfassembled peptide nanotubes. *Science*, *300*, 625-627.

125. Patolsky, F.; Weizmann, Y.; Willner, I. (2004) Actin-based Metallic Nanowires as Bio- nanotransporters. *Nat. Mater. 3*, 692-695.

126. Behrens, S.; Habicht, W.; Wagner, K.; Unger, E (2006). Assembly of nanoparticle ring structures based on protein templates. *Adv. Mater.*, *18*, 284-289.

127. Bhattacharya, R.; Patra, C. R.; Wang, S. F.; Lu, L. C.; Yaszemski, M. J.; Mukhopadhyay, D.; Mukherjee, P. (2006), Assembly of Gold Nanoparticles in a Rodlike Fashion sing Proteins as Templates. *Adv. Funct. Mater, 16*, 395-400.

128. Anamika Mubayi, Sanjukta Chatterji, Prashant M. Rai, Geeta Watal (2012)," Evidence based Green Synthesis of Nanoparticles", *Advanced Materials Letters*, 3(6), 519-525.